Right ventricular volume load and function in congenital heart defects

Sverrir Stephensen, Sigurdur

2017

Document Version:
Publisher's PDF, also known as Version of record

Right ventricular volume load and function in congenital heart defects

SIGURÐUR SVERRIR STEPHENSEN
DEPARTMENT OF CLINICAL PHYSIOLOGY | LUND UNIVERSITY

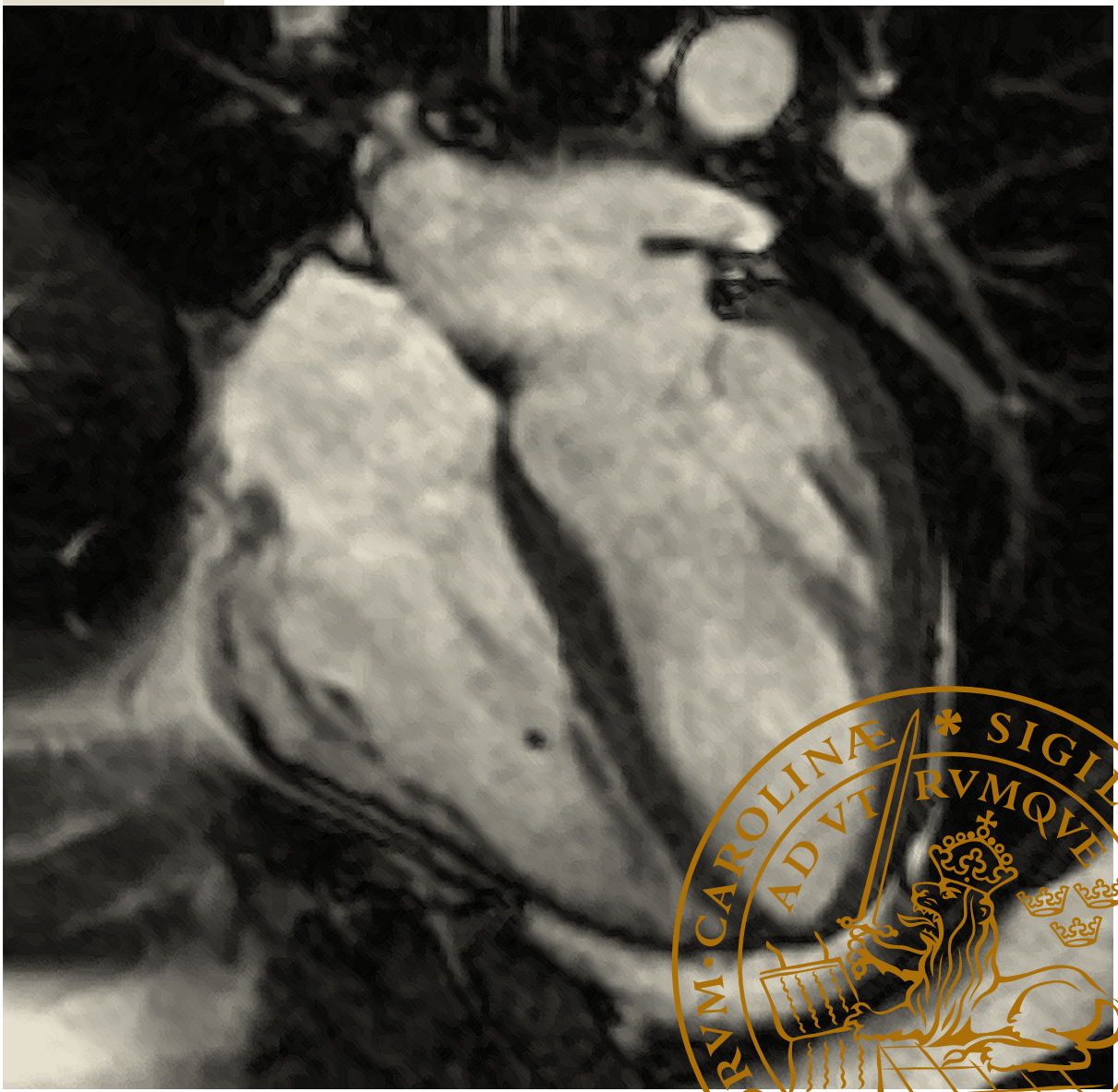

Right ventricular volume load and function in congenital heart defects

Lund University, Faculty of Medicine Doctoral Dissertation Series 2017:182

Right ventricular volume load and function in congenital heart defects

Sigurður Sverrir Stephensen

LUND
UNIVERSITY

DOCTORAL DISSERTATION
by due permission of the Faculty of Medicine, Lund University, Sweden.
To be defended at föreläsningssal 2, Skåne University Hospital, Lund on
Wednesday, 13th of December 2017 at 09:00.

Faculty opponent
Dr Sonya Babu-Narayan
Royal Brompton Hospital, Sydney Street, London, UK

Organization
LUND UNIVERSITY
Department of Clinical Physiology
Skåne University Hospital, Lund
SE-22185 Lund, Sweden

Document name:
Doctoral Dissertation

Date of issue
2017-11-07

Author(s): Sigurður Sverrir Stephensen

Sponsoring organization
Swedish Research Counsil, Swedish Heart and Lung Foundation, Medical Faculty at Lund University, Region of Scania

Title and subtitle. Right ventricular volume load and function in congenital heart defects.

Right ventricular (RV) volume load is the effect of different types of congenital heart defects (CHD) like tetralogy of Fallot, secondary to pulmonary regurgitation (PR), and atrial septal defect (ASD) because of left-to-right shunt. Dilatation of the RV leads to bulging of the ventricular septum into the left ventricle in diastole and alters the normal cardiac pumping mechanisms. Understanding how pumping mechanics differ between health and disease and how they adapt to different loading conditions is important in the assessment of patients with different etiology for RV volume load and for the development of new treatment for RV dysfunction. Patients with ASD can be asymptomatic at rest but show impaired exercise tolerance during stress. It is therefore important to study cardiac pumping during stress since it may provide insight into why people with the same type of heart defect and similar RV volume load can have different clinical symptoms. The aim of the thesis was to study pumping mechanics in patients with different eatiology for RV volume load, compare them to healthy subjects and examine what changes occur during stress as well as during the first year after repair of the heart defect.

Study I showed that PR leads to paradoxical septal motion that contributes to RV stroke volume (SV) instead of left ventricular SV. Longitudinal contribution to RVSV is decreased and lateral contribution to RVSV is increased. This leads to better matching between atrioventricular plane displacment inflow of blood to the right side of the heart. In healthy subject the septum contributes to 7% of LVSV.

Study II revealed that in patients with ASD, pulmonary-to-systemic flow ratio (QP/QS) and left-to-right shunt per heart beat is decreased during stress. High systemic cardiac output during stress is strongly related to exercise capacity in ASD patients. On day one after transcutaneous ASD closure RV remodelling has already started with the septum contributing to LVSV.

Study III compared cardiac pumping in patients with RV volume load due to ASD and PR. It revealed that pumping mechanics depend on the etiology for the RV dilatation rather than degree of RV size. Regional contribution to SV in ASD patients is similar to healthy subjects but differs from patients with PR.

Study IV is a follow-up study after transcutaneous closure of ASD. It showed that quantification of shunt size or ventricular volumes during stress did not predict exercise capacity 12 months after transcutaneous ASD closure. Improvement in aerobic capacity after ASD closure was subtle and patients with smaller QP/QS before closure had larger improvement in predicted aerobic capacity at follow-up.

Key words. Right ventricular volume load, congenital heart defects, magnetic resonance imaging, exercise tolerance

Classification system and/or index terms (if any)

Supplementary bibliographical information | Language: English

ISSN and key title 1652-8220 | ISBN 978-91-7619-564-2

Recipient's notes | Number of pages | Price

Security classification

Signature  Date 2017-11-07

Right ventricular volume load and function in congenital heart defects

Sigurður Sverrir Stephensen

LUND
UNIVERSITY

Doctoral Dissertation 2017

Department of Clinical Physiology
Lund University, Sweden

Coverphoto: Magnetic resonance image showing a four-chamber view of the heart in end-diastole.

ssstephensen@gmail.com

Faculty of Medicine
Department of Clinical Physiology

ISBN 978-91-7619-564-2
ISSN 1652-8220

Printed in Sweden by Media-Tryck, Lund University
Lund 2017

There is water on the bottom of the ocean

"Once in a lifetime" by Talking Heads

I have a motto: It's never too late to give up.
It's never too late to give up what you
are doing, and start doing what you realize you love.

Hans Rosling

Content

Summary

Right ventricular (RV) volume load is the effect of different types of congenital heart defects (CHD) like tetralogy of Fallot, secondary to pulmonary regurgitation (PR), and atrial septal defect (ASD) because of left-to-right shunt. Dilatation of the RV leads to bulging of the ventricular septum into the left ventricle in diastole and alters the normal cardiac pumping mechanisms. Understanding how pumping mechanics differ between health and disease and how they adapt to different loading conditions is important in the assessment of patients with different aetiology for RV volume load and for the development of new treatment for RV dysfunction. Patients with ASD can be asymptomatic at rest but show impaired exercise tolerance during stress. It is therefore important to study cardiac pumping during stress since it may provide insight into why people with the same type of heart defect and similar RV volume load can have different clinical symptoms.

Study I showed that PR leads to paradoxical septal motion that contributes to RV stroke volume (SV) instead of left ventricular SV. Longitudinal contribution to RVSV is decreased and lateral contribution to RVSV is increased. In healthy subject the septum contributes to 7% of LVSV.

Study II revealed that in patients with ASD, pulmonary-to-systemic flow ratio (QP/QS) and left-to-right shunt per heart beat is decreased during stress. High systemic cardiac output during stress is strongly related to exercise capacity in ASD patients.

Study III compared cardiac pumping in patients with RV volume load due to ASD and PR. It revealed that pumping mechanics depend on the aetiology for the RV dilatation rather than degree of RV size. Regional contribution to SV in ASD patients is similar to healthy subjects but differs from patients with PR.

Study IV is a follow-up study after transcutaneous closure of ASD. It showed that quantification of shunt size or ventricular volumes during stress did not predict exercise capacity 12 months after transcutaneous ASD closure. Patients with smaller QP/QS had larger improvement in predicted exercise capacity at follow-up.

Populärvetenskaplig sammanfattning

Medfött hjärtfel drabbar ungefär en procent av alla levande födda barn. Hjärtfelen blir i de flesta fall diagnosticerade under det första levnadsåret men det finns även medfödda hjärtfel som inte upptäcks förrän i vuxen ålder. Symptomen varierar och kan t.ex. orsaka cyanos, varvid syrefattigt och syrerikt blod blandas i blodomloppet p.g.a. hjärtfelet, men även visa sig bara som andfåddhet, trötthet och hos barn dålig viktuppgång. Ett av de vanligaste hjärtfelen kallas förmaksseptumdefekt (ASD) och innebär ett hål i skiljeväggen mellan förmaken. Hålet orsakar ett shuntflöde av syrerikt blod från vänster förmak över hålet tillbaks till det syrefattiga högra förmaket. Den ökade mängden blod som återkommer till höger förmak orsakar en förstoring och en volymbelastning av de högersidiga hjärtrummen och samtidigt även fyller ut lungpulsådern och dess förgreningar till lungorna.

Ett annat medfött hjärtfel som också kan orsaka volymsbelastning av höger kammaren kallas Fallots tetralogi. Hjärtfelet behöver i allmänhet opereras. Efter operation kan det uppstå ett läckage i lungpulsåderklaffen som gör att höger kammare kommer att belastas med större volymer blod.

Syftet med avhandlingen var att studera hjärtfunktionen med magnetkamera (MR) i dessa två patientgrupper med volymbelastning av högerkammare, jämföra dem med friska personer och granska om högerkammarens funktion ändras vid belastning. Dessutom at följa upp patienterna med ASD med upprepade MR och arbetsprov i 12 månader efter ASD slutning.

Delarbete I visade att hos friska personer bidrar kammarskiljeväggen med 7% till vänsterkammares slagvolym (SV). Läckage i lungpulsåderklaffen orsakar paradoxal förskjutning av kammarskiljeväggen som bidrar till högerkammares SV i stället för att bidra till vänsterkammares SV. Det längsgående bidraget till högerkammares SV är minskat och det radiella bidraget är ökat.

Delarbete II visade att hos patienter med ASD ändrar sig vid fysisk ansträngning, relationen mellan blodflödet som skall nå lungorna och det som skall nå ut i resten av kroppen. Det betyder att med ökad hjärtfrekvens minskar flödet över förmaksseptumdefekten medan flödet från vänster förmak till vänster kammare ökar. Högt flöde i kroppspulsådern kan knytas till en god arbetsförmåga hos patienter med ASD.

Delarbete III jämförde hjärtfunktionen i patienter med läckage i lungpulsåderklaffen och ASD. Studien visade att det är orsaken till volymbelastningen snarare än storleken på högerkammaren, som avgör på vilket sätt hjärtat pumpar blod. Den regionala hjärtfunktionen hos ASD patienter liknar den hos friska.

Delarbete IV är en uppföljningsstudie efter ASD-slutning med kateterteknik. Den visade att varken storleken på shunten över förmaksseptumdefekten eller högerkammares storlek under stress kunde förutse arbetsförmågan 12 månader efter slutning av defekten. Patienter med relativt litet shunt visade större förbättring i arbetsförmåga efter slutning.

Abbreviations

ASD	Atrial septal defect
AVPD	atrioventricular plane displacement
AV-plane	atrioventricular plane
BSA	body surface area
CHD	congenital heart defects
CI	cardiac index
CMR	cardiac magnetic resonance
CO	cardiac output
COV	center of volume
COVV	center of volume variation
ECG	electrocardiography
ED	end-diastole
EDV	end diastolic volume
EF	ejections fraction
ES	end-systole
ESV	end systolic volume
LA	left atrium
LV	left ventricle
LVEDVI	left ventricular end diastolic volume indexed to body surface area
LVESVI	left ventricular end systolic volume indexed to body surface area
LVSV	left ventricular stroke volume
MRI	magnetic resonance imaging
NYHA	New York heart association
PAH	pulmonary artery hypertension
PR	pulmonary regurgitation
PVR	pulmonary valve replacement
QP/QS	pulmonary to systemic flow ratio
RA	right atrium
RF	radiofrequency
RV	right ventricle
RVEDVI	right ventricular end diastolic volume indexed to body surface area
RVESVI	right ventricular end systolic volume indexed to body surface area
RVSV	right ventricular stroke volume
SV	stroke volume
TAPSE	tricuspid annular plane systolic excursion
TEE	trans esophageal echocardiography
THVV	total heart volume variation
TOF	tetralogy of Fallot
TR	tricuspid regurgitation

VENC	velocity encoding gradient
VO_2 peak	peak oxygen uptake
VO_2 %	VO_2 peak percent of predicted value
VSD	ventricular septal defect

1. Introduction

1.1 Congenital heart defects

Heart defects are the most common congenital anatomical defects with around one percent of children born with a heart defect (53). Congenital heart defects (CHD) are often divided into three categories based on their clinical symptoms; 1. left-to-right shunting with increased pulmonary blood flow, 2. cyanotic heart defects, where pulmonary blood flow is often decreased and 3. obstructive lesions. The right ventricle (RV) is often affected in CHD and can be the subject of volume load, pressure load or both.

1.2 Atrial septal defect

One of the most frequent CHD causing volume load on the RV is atrial septal defect (ASD) (Figure 1.1) where the septum, separating the two atria, has not fused during fetal life. This allows oxygenated blood to be shunted from the left to the right atrium. The right ventricle (RV) is more compliant than the left ventricle (LV), reflecting the low resistance of the pulmonary vasculature compared to the systemic circulation. This leads to blood shunting from left to right across the ASD. From the right atrium (RA) the blood flows through the tricuspid valve and into the right ventricle and onwards to the lungs. The left-to-right shunting causes volume overload and dilation of the right heart chambers. ASD is often not diagnosed until adulthood since clinical signs and symptoms can take decades to evolve. Indications for ASD closure are RA or RV enlargement with or without symptoms such as

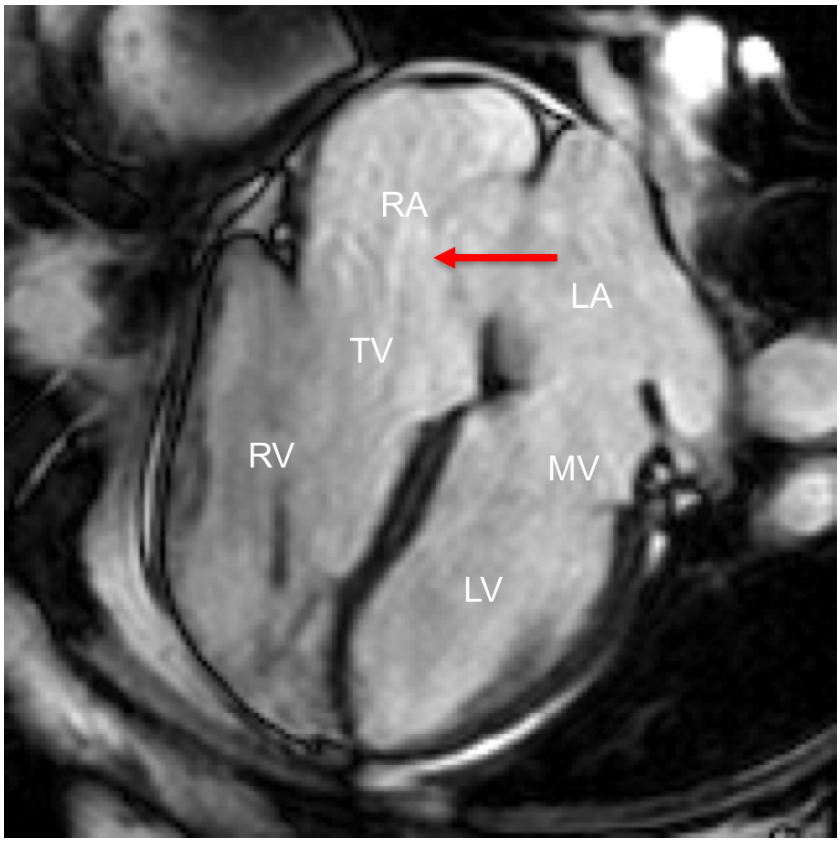

Figure 1.1
Four chamber view in end-diastole showing secundum atrial sepetal defect. Red arrow shows the direction of the shunt from the left atrium (LA) to the right atrium (RA). The shunt has caused dilation of the right ventricle (RV). LV; left ventricle, TV; tricuspid valve, MV; mitral valve.

dyspnea, fatigue, palpitations and exercise intolerance, given that pulmonary artery pressure is less than 2/3 of systemic pressure. Pulmonary to systemic flow ratio (QP/QS) is often used to evaluate the hemodynamic significance of an ASD. A ratio of 1,5 or more is considered large enough to cause overload of the right-sided heart chambers. Other indications for ASD closure are paradoxical embolism causing stroke or transient ischemic attack.

1.3 Tetralogy of Fallot

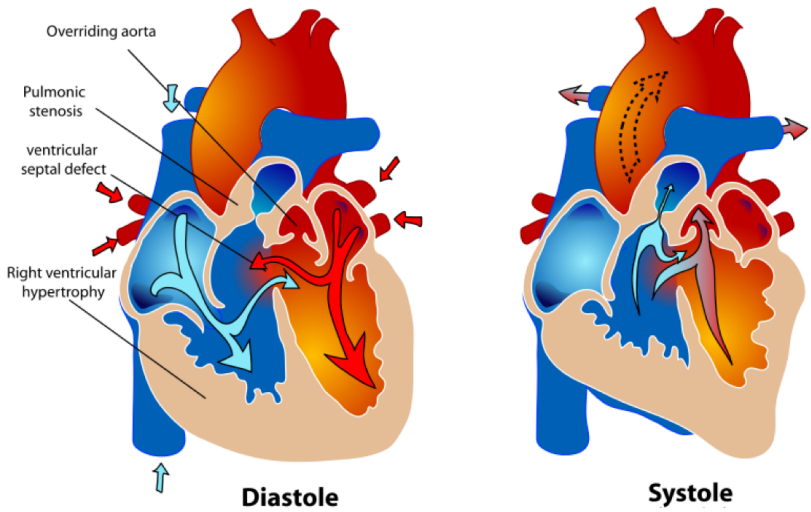

Figure 1.2
Tetralogy of Fallot with pulmonary stenosis, ventricular septal defect (VSD), overriding aorta and right ventricular (RV) hypertrophy. In systole there is a right-to-left shunting of deoxygenated blood over the VSD and out to the aorta, secondary to the obstruction in the RV outflow tract and the pulmonary valve.

Tetralogy of Fallot (TOF) is the most common cyanotic heart defects. It involves four components; a subpulmonary valve stenosis, a ventricular septal defect (VSD), an aorta that overrides the ventricular septum and a hypertrophic RV (Figure 1.2). The pulmonary valve is often underdeveloped. As with other complex heart defects, children with TOF can be diagnosed prenatally but more often they present soon after birth with cyanosis. The pulmonary valve stenosis causes pressure load on the RV and a right-to-left shunt through the VSD with desaturated blood entering the systemic circulation (Figure 1.2). Granted that the infundibular or pulmonary valve stenosis is not critical, causing severe cyanosis, the correction of TOF usually takes place at 3-6 months of age. It includes relieving the stenosis of the pulmonary valve, often through infundibular resection and insertion of transannular patch and closure the VSD with a gore-tex patch (Figure 1.3).

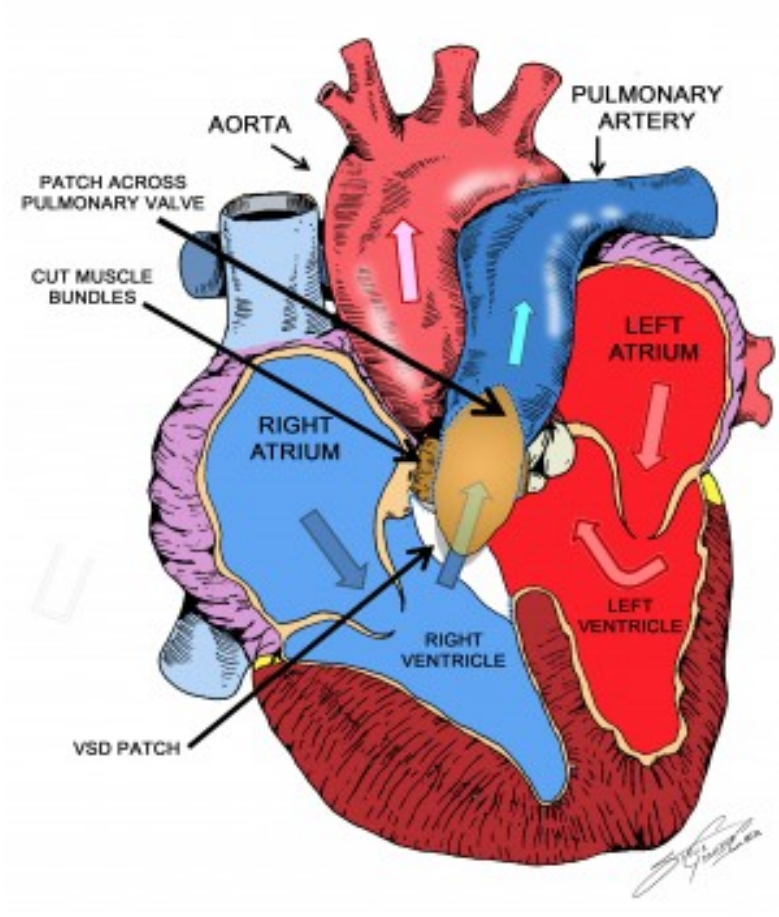

Figure 1.3
Surgical repair for tetralogy of Fallot includes releive of infundibular and pulmonary stenosis, often with the use of transannular patch and closure of the ventricular septal defect (VSD) with a patch.

1.4 The left and right ventricle

The LV is thick-walled, stiff and cylinder shaped with compact endocardium, whereas the RV is thin-walled with trabeculations, compliant and wrapped around the LV anterolaterally. The different morphology reflects their function with the LV pumping blood to the high-pressure systemic circulation and the RV pumping blood to the low-pressure system of the pulmonary vascular bed. The right and left ventricles originate from different embryological precursor cells (106), which may be related to their different form and structure and can explain different response to

abnormal loading conditions (26, 38). The myocytes are oriented radially in the midlayers of the LV but have helical configuration in the subepicardial and subendocardial layers. The RV has primarily longitudinal myocyte orientation. Even though the ventricles have different morphology and function they are tightly coupled through the electrical conduction system, the pericardium (19, 47) and common myocardial fibers and the interventricular septum as elegantly presented on diffuse tensor MR images in a study by Smerup et al (87) (Fig 1.4). Therefore, abnormal pressure- or volume loading condition of either ventricle directly affects the filling and contraction of the other.

Figure 1.4
Short axis image of the left and right ventricles. Myofibers cross from the parietal walls of the left ventricle to the right ventricle. *Reprinted from Smerup ete al.* (87) *with permission from John Wiley and Sons.*

Longitudinal function is the movement of the atrioventricular plane (AVP) towards the apex in systole (55). The RV contracts predominantly in the longitudinal direction with the AVP contributing to approximately 80% of RV stroke volume (SV) and 20% contributed from the radial displacement of the lateral wall (15). On the left side, the AVP displacement contributes to 60% of the LVSV (15) and the rest is derived from the inward movement of the lateral wall (~32%) and the ventricular septum (~8%)(90). Since the septum moves towards the LV and away from the RV in systole, its' motion has a negative effect on the RV contraction. The RV longitudinal and lateral wall motion must compensate for the loss of septal contribution to the RVSV.

1.5 Right ventricular pressure and volume load

Increased afterload, as seen in severe pulmonary valve stenosis or pulmonary hypertension, leads to RV hypertrophy. However, since there is individual variation in the degree of hypertrophy with the same degree of afterload it has been suggested that there might be genotypic difference between patients in how the RV responds to stress (103). RV remodeling is thus divided into "adaptive remodeling" with preserved systolic and diastolic function and "maladaptive remodeling" with dilatation and impaired ejection fraction (101). RV hypertrophy that signifies a normal physiological adaption in diseases such as Eisenmenger syndrome can be pathological in other diseases, such as pulmonary arterial hypertension (PAH), and linked to increased mortality (42). The underlying pathological condition is thus of more importance in assessing morbidity than the RV hypertrophy per se. Tissue fibrosis of the RV is a significant feature in animal models with maladaptive RV hypertrophy, but less evident in cases of adaptive RV hypertrophy (101).

Volume overload of the RV is better tolerated than pressure overload, with better preserved exercise tolerance (4). In study by Bartelds et al RV end-diastolic volume (EDV), RV end-systolic volume (ESV) and RV stroke volume (SV) were increased and genetic expression was different in mice with RV volume load compared to mice with pressure load (4). The stroke work of mice with RV pressure load was higher which might lead to RV failure in a shorter time. Just as with RV pressure load, RV volume load is related to the underlying pathological condition. Patients with TOF often undergo open heart surgery at an early age as previously described. This is done under general anesthesia on cardiopulmonary bypass. These patients may have a gore-tex patch in the ventricular septum and the RV outflow tract. CMR in TOF patients has revealed fibrosis not only at these two sites and at the RV insertion points of the ventricular septum, but also in sites remote from surgical incision (3, 93). RV fibrosis has even been detected in experimental animal model with aortocaval shunt leading to RV volume load without prior cardiac surgery (62). Most patients with RV volume load and some patients with pressure load have paradoxical septal motion, i.e. the ventricular septum moves to the right in systole, contributing to RVSV instead of LVSV as in healthy subjects (67, 90). In diastole the septum moves back to the left and can affect the LV filling (92).

1.6 Imaging and evaluating right ventricular function

Because of its' complex morphology, the RV is more difficult to visualize on echocardiography than the LV and evaluation of RV function is more challenging. Tricuspid annular plane systolic excursion (TAPSE) is easy to measure on echocardiography and is used to assess regional longitudinal function. Tissue Doppler velocity imaging of the tricuspid annulus is an alternative for evaluation of longitudinal RV motion. Strain imaging is used to measure regional myocardial shortening and lengthening or thickening and thinning and strain rate measures the rate of this deformation over time. Strain and strain rate measurements give information on myocardial contractility and their use is growing (60). Cardiac magnetic resonance (CMR) is the imaging method of choice for studying ventricular volumes and mass, stroke volume, ejection fraction and flow and to quantitate valve regurgitation (1, 5, 81). With serial studies the progression of RV volumes and pulmonary regurgitation can be followed over time. This is especially important in patients with TOF and ASD where RV dilatation can signal the progress of RV dysfunction (60). Further information on the extent and location of myocardial fibrosis, a prognostic factor in TOF patients, can be obtained by using delayed contrast enhancement (3).

1.7 Treatment

Today the closure of ASD secundum is most often done transcutaneously with a device as described in figure 1.5. If not feasible the defect is closed in an open heart surgery using cardiac bypass. ASD closure is generally favorable with receding symptoms and improved exercise capacity (7, 35, 36, 43, 96), but that is not true for all patients (72, 75, 83). In patients with TOF who have developed significant pulmonary regurgitation as a consequence of the subpulmonary and pulmonary valve resection, the timing and indications for treatment with pulmonary valve replacement is not as clear-cut. The nature of the disease is such that surgical treatment seldom proves sufficient in the long run. Incompetent pulmonary valve and RV dilatation have traditionally been surgically corrected by inserting a conduit, with stented bioprosthetic valve, from the RV to the pulmonary artery.

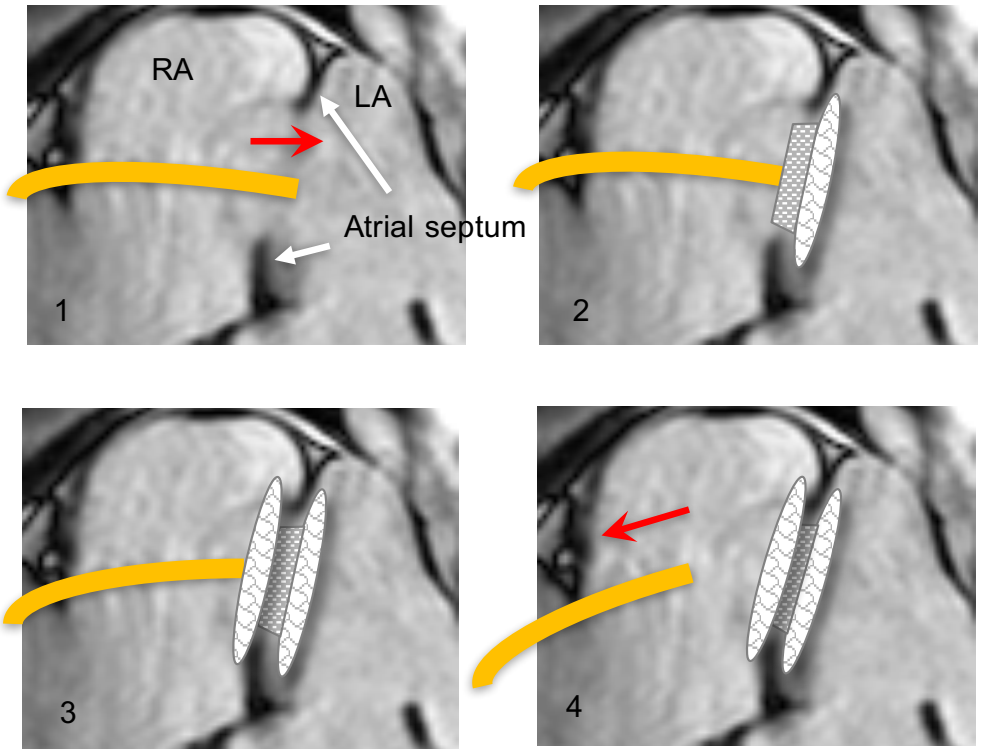

Figure 1.5
Transcutaneous ASD closure. 1. A catheter containing ASD closure device is inserted through the inferior vena cava into the right atrium (RA) and through the ASD (red arrow). 2. With the tip of the catheter in the left atrium (LA) the left disc of the device is opened. 3. The catheter is pulled back into the RA and the right disc is opened. 4. If the device is stable and properly positioned it is detached and the catheter is removed.

The lifetime of such a conduit is around 10 years but during that time the prosthetic valve tends to calcify and starts to leak causing the RV to dilate again requiring a new pulmonary valve replacement (PVR). Indications for such a procedure have been based on the amount of pulmonary regurgitation (PR), RV function and RV size indexed to body surface are (BSA), but the cut off values have been debatable. The current guidelines recommend PVR if RV end diastolic volume indexed to BSA (RVEDVI) is > 150 ml/m^2 (10)(33), RV end systolic volume indexed to BSA (RVESVI) is > 90 ml/m^2 (33), RV ejection fraction < 47% or QRS duration > 140 ms in asymptomatic patients (33). Symptoms thought to be secondary to RV overload such as exercise intolerance, dyspnea, peripheral edema or other signs of heart failure and syncope secondary to arrhythmia are also indications for PVR in TOF patients. Long term survival of TOF patients is excellent but increased risk of arrhythmia (28) and sudden death and has been documented with survival over 25 years postoperatively (65, 102).

1.8 Magnetic Resonance Imaging

Magnetic resonance imaging (MRI) is a complex imaging technique that uses magnetic fields, radiofrequency and field gradient to create images of anatomical structures. The magnetic field affects hydrogen ions (H^+) that are a part of water (H_2O), which makes up to 70% of human tissues. Hydrogen ions or protons have a positive electrical charge and each proton can be seen as a small electric charge that rotates or spins around a magnetic field axis. The direction, frequency, magnitude and phase of the spinning can be altered in order to create images. It is thus the patient's own tissues that respond to external stimuli to create images. When a patient lies in the MR scanner the magnetic field makes most of the protons spin in the direction of the magnetic field. However, some protons align in the opposite direction of the magnetic field. The protons that spin in the opposite directions cancel each other out so that in the end we are left with one vector that is the sum of all the magnetic vectors. This vector points in the direction of the magnetic field, is parallel to it and can therefore not be measured. However, this is the vector we would like to measure and to be able to do so we use radiofrequency pulse to change the direction of the protons. By altering the direction of the protons so that they all spin in the same direction at the same time, we create a new magnetic vector. When the radiofrequency (RF) pulse is switched off the protons start relaxing and spin out of phase. By constantly changing this magnetic vector we can create an electric current which is picked up by a RF receiver. Gradient coils are used to spatially locate an MR signal. They create inhomogeneity in the magnetic field and spatially encode a specific slice of tissue. The signal detected by the RF receiver is collected in the so-called k-space. The k-space holds the raw data which later is reconstructed into images.

What makes cardiac MR more challenging than imaging of other tissues is not only the movement of the heart and the blood in and out of the organ, but also the respiratory movement of the thorax. To reduce the effect of moving structures, ECG gating is used to synchronize image acquisition and imaging is performed during end expiratory breath hold. Cine images are acquired using steady state free precession sequence covering the whole heart from the apex to the base. ED and ES volumes for the left and right ventricle are determined by delineating the endocardial border in all slices in ED and ES. Stroke volume is calculated as the EDV – ESV. Since this method only compares the volume inside the ventricle in ED and ES it is inaccurate method in patients with moderate to severe valve leakage such as in patients with pulmonary regurgitation. A more accurate method for determining the effective stroke volume (SV – regurgitated volume) is flow imaging. Phase contrast technique relies on changes in the magnetization of blood flow in cross section of the vessel of interest. Changes in the phase of the blood's magnetization are detected and thus information on forward and backward flow are collected. A plane,

perpendicular to the flow direction in a vessel is defined and the SV and the backward flow are measured. By subtracting the backward flowing blood volume from the SV, the effective SV is calculated. This method is used to calculate the absolute volume and percent of pulmonary regurgitation in patients with PR as well as left-to-right shunting in ASD patients, by comparing the flow in the aorta and the pulmonary trunk.

The strength of a magnetic field is expressed in units of magnetic flux density which is called tesla (T). The magnetic field is always on and the magnet needs constant cooling down. Most scanners have superconducting magnets with magnetic field of 0.5 T or higher and in CMR 1.5 to 3.0 T is most commonly used.

2.Aims

The aims of the thesis were to study the right ventricular function in patients with RV volume load at rest and during stress with MRI and to examine if left-to-right shunting during stress is related to outcome after transcutaneous ASD closure.

The specific aims of each paper were:

I. to quantify the longitudinal, lateral and septal contribution to stroke volume in children and adults with right ventricular volume load secondary to pulmonary regurgitation and compare the results to healthy controls.

II. to determine if systemic and pulmonary flow, left-to-right shunting and ventricular volumes in ASD patients change during stress and if these changes are related to aerobic capacity.,

III. to quantify the regional contribution to stroke volume in patients with ASD at rest, during dobutamine stress and after transcutaneous ASD closure and to compare the results to patients with RV volume load secondary to pulmonary regurgitation.

IV. to study if left-to-right shunting and ventricular function during dobutamine stress in patients with ASD is a better prognostic factor for exercise capacity 12 months after transcutaneous closure of the ASD than studies at rest and to determine the time-course of ventricular remodelling following transcutaneous ASD closure.

3. Materials and methods

3.1 Study population

Study I

Two groups of patients were studied: 15 children (8 females) and 15 adults (6 females) who had undergone corrective surgery for TOF or pulmonary stenosis. The patients had varying degree of pulmonary regurgitation (PR) from 0 to 61%. RV systolic pressure was calculated from the maximum velocity of the tricuspid regurgitation (TR) jet on echocardiography according to the simplified Bernoulli equation (Pressure gradient = 4 times velocity squared) (39). Effective RVSV was calculated by subtracting the PR volume, obtained from the flow analysis, from the RVSV obtained from the short-axis cine images (RVEDV-RVESV). Nine healthy children (3 females) and 45 healthy adult volunteers (25 females) with varying degrees of exercise level, to obtain a wide range of heart volumes, were used as controls.

Study II-IV

Nineteen patients (13 females) with hemodynamically significant ASD, based on clinical findings, echocardiography and CMR were included and eight patients (3 females) with small ASD, not eligible for closure. Sixteen healthy volunteers (3 females) were included as well. Seventeen patients with large ASD, the 8 patients with small ASD and all of the controls underwent dobutamine-atropine stress. Patients with uncontrolled atrial fibrillation were excluded from the dobutamine stress. In 17 patients, the ASD was closed transcutaneously. Two patients underwent open heart surgery for ASD closure and were excluded from follow-up studies as well as one patient who died a few months after the transcutaneous ASD closure.

In study II, 16 patients with large ASD and 4 patients with small ASD were included. They were presented together as a group (N=20) to study the relation between ASD size and left-to-right shunting. The patients were 24-81 years old and there were 15 females. CMR was done at rest and during dobutamine stress.

In study III, nineteen patients (mean age 50 years, 13 females) with large ASD underwent CMR at rest and 17 of those during dobutamine stress. The day after transcutaneous closure 16 patients underwent CMR at rest. The group of controls from study II was reduced to 10 subjects to better match the age and gender of the patient group. Patients with small ASD were not included. The cohort of 30 patients with RV volume load and PR from study I was included for comparison.

In study IV, seventeen patients were scheduled for CMR 3 and 12 months following transcutaneous ASD closure. One patient refused the 12 months follow-up and was excluded from the previous studies as well, leaving 16 patients (mean age 52 years, 11 females) for inclusion. Exercise testing was done at 12 months follow-up in 15 patients.

3.2 MRI scanners and sequences

A 1.5T CMR scanner was used for all studies (Philips Achieva, Best, The Netherlands) except for one 12 months follow-up study (Siemens, Aera, Erlangen, Germany). Steady state free precession cine CMR images were acquired at rest and during dobutamine stress in short-axis planes covering the entire heart and long axis images in 2-chamber, 3-chamber and 4-chamber views. Imaging parameters for cine CMR on the Philips scanner were typically: retrospective ECG triggering with acquired temporal resolution of 47 ms reconstructed to 30 time phases per cardiac cycle, repetition time 3 ms, echo time 1.4 ms, flip angle 60°, and slice thickness 5-8 mm with no slice gap. Breath-hold times were typically 10s. The only study done on the Siemens scanner had similar settings. Flow velocity mapping of the aorta and pulmonary trunk in ASD patients was acquired at rest and during dobutamine stress using a retrospective ECG triggered fast-field echo velocity encoded sequence, acquired during free breathing. Imaging parameters were typically: repetition time 10 ms, echo time 5 ms, flip angle 15°, and slice thickness 8 mm, acquired in-plane resolution 2.4 x 2.4 mm reconstructed to 1.3 x 1.3 mm, number of acquisitions 1, no parallel imaging and a velocity encoding gradient (VENC) of 200 cm/s. The VENC was increased to 280 cm/s during dobutamine stress if needed. The flow sequence had an acquired temporal resolution of 20 ms during the cardiac cycle reconstructed to 35 phases per heart cycle and a typical scan time of 2 minutes at rest. The same parameters were used for the pulmonary trunk in TOF patients with pulmonary regurgitation. The flow sequence had been previously validated in vivo and in vitro (11).

3.3 Dobutamine-atropine stress test

Exercise testing during CMR study has proved challenging. The patient has to lie still in the MR scanner to avoid artefacts but at the same time be able to exercise sufficiently to increase heart rate and stroke volume. It has also been difficult to obtain good ECG signal for ECG gating during exercise. Therefore, medications have been used to simulate the physiological response of the cardiovascular system during exercise. Dobutamine is a strong beta-1 agonist, a moderate alfa-agonist and a weak beta-2 agonist. It improves cardiac contractility and thus increases stroke volume, leads to increase in heart rate and a mild elevation of blood pressure (99). Dobutamine seems to have little effect on the pulmonary circulation (68). Atropin has anticholinergic effect through vagal inhibition and increases the heart rate. During physical exercise SV increases by around 30% and heart rate by 150%. Dobutamine has primarily been used in stress echocardiography, CMR and myocardial scintigraphy (17, 51, 69). Known side effects are headache, hypertension, chest pain and tachycardia, nausea and anxiety (51). Atropine is frequently used to increase heart rate. Side effects include dry mouth, urinary retention, excitement and disorientation (29, 61, 86). Intravenous infusion of 10 µg/kg/min of dobutamine for 3 minutes followed by 20 µg/kg/min dobutamine was administered and 0.25-0.75 mg atropine was added to reach a target of 70% of age-predicted maximal heart rate determined as 220 minus the patient's age. The most obvious limitation of medically induced stress compared to physical exercise is the lack of muscle pumping of the lower extremities, which affects venous return to the heart.

3.4 Right heart catheterization and transcutaneous ASD closure

Right heart catheterization was done in general anaesthesia and intracardiac pressures were measured using 5F MPA catheter in the left and right atria, right ventricle and pulmonary artery before ASD closure. Amplatzer^{TM} septal occluder, which is MRI safe, was used in all patients. A catheter is inserted from the right atrium (RA) through the ASD and into the left atrium (LA). The left sided disc is opened up and pulled against the septum. With the tip of the catheter now in the RA the right sided disc is opened up so the double disc now covers the ASD on both sides (Figure 1.5). Transoesophageal 2-dimensional echocardiography (TEE) was performed using Philips iE33 (The Netherlands) with X7-2t or T6H probes during the procedure. The diameter of the ASD was measured in two imaging planes without balloon inflation. The cross-sectional area of the ASD was calculated using

the formula for ellipse (π x radius1 x radius2). Residual shunt is not uncommon following transcutaneous closure of ASD but it usually resides in a few months.

3.5 Ergospirometry

Exercise testing was performed using Monark 939E cycle ergometer and Oxygen Pro (Jaeger, Hochberg, Germany) was used to determine peak oxygen uptake (VO_2 *peak*). The test protocol was chosen based on the age and sex of the patient with workload starting at 30-50 W and increased by 10-20 W per minute. VO_2 was measured breath by breath and reported as the average of each 10 seconds interval. VO_2 *peak* was defined as the average of the three highest VO_2 values documented during the last minute of the test. The test was discontinued upon exhaustion. Blood pressure and a 12 lead ECG were monitored during exercise. VO_2 *peak percent* of predicted value (VO_2 *%*) was calculated according to the Hansen/Wasserman equation (104).

3.3 Image analyses

CMR images in all studies were analyzed using Segment (v 1.9-2.0), a freely available software (http://segment.heiberg.se). Left and right ventricular SV were obtained by delineating the endocardial border of both ventricles in all slices from the base to the apex in end-diastole and end-systole.

3.3.1 Longitudinal contribution to stroke volume

Longitudinal contribution to SV for each ventricle was calculated as previously validated (15, 16). In short, the position of the atrioventricular plane was determined by using eight location points in the three long axis images, 2-chamber, 3-chamber and 4-chamber view (Figure 3.1). The atrioventricular plane displacement (AVPD) was calculated for each ventricle by subtracting the AVP position in ES from that in ED. The mean of the two to three largest epicardial short-axis areas of the LV and the RV encompassed by the AVPD was multiplied by the AVPD to calculate the volume contributed to SV by the AVPD. The reason for using the epicardial area has been described by Carlsson et al. (16) by comparing the LV to a telescope, which shortens and lengthens along its long axis. On shortening, the telescope retains its

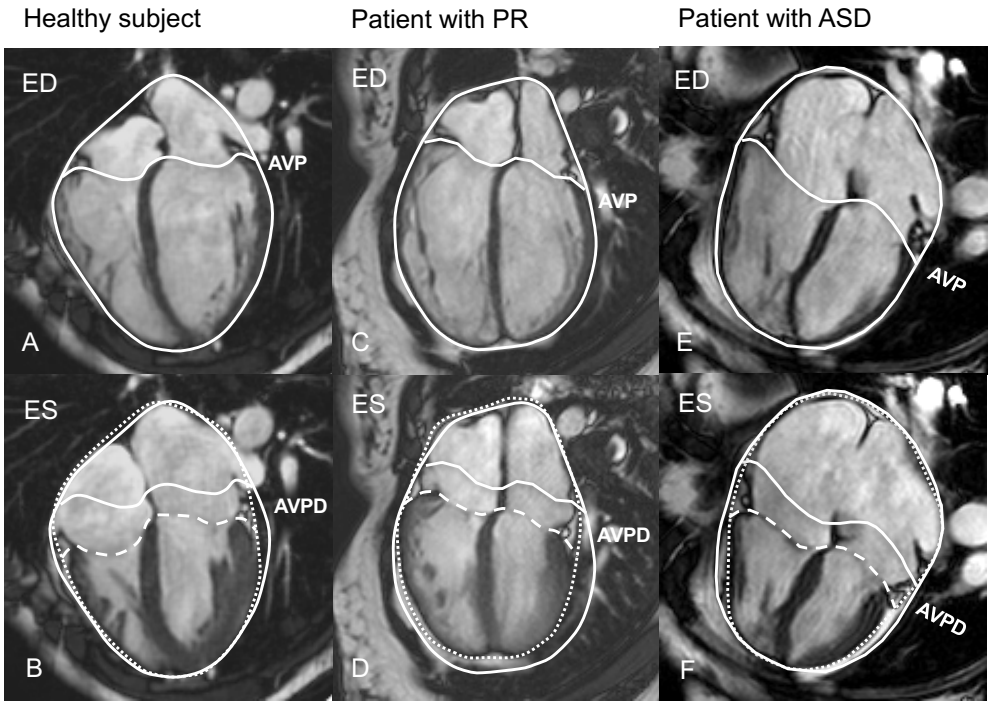

Figure 3.1
Cardiac MR images in the 4-chamber view in a healthy volunteer (A, B), and two patients with RV volume load; a patient with severe PR secondary to tetralogy of Fallot (C,D) and a patient with ASD (E, F). The solid and the dotted lines represent the pericardial contours in end-diastole (ED) and end-systole (ES), showing the outer volume variations between ED and ES. The atrioventricular plane (AVP) is seen as a solid vertical line in ED and a dotted vertical line in ES. The AVP displacement (AVPD) is the distance between the solid and the dotted vertical lines shown in ES.

outer diameter but the inner diameter decreases. The volume of the telescope decreases when the tube shortens. Likewise, the volume of the ventricle decreases and this volume equals the SV. As the AVP is pulled towards the apex the myocardium gets rearranged, but the myocardial volume is constant during the cardiac cycle. The only difference in volume between ED and ES is what was inside the tube or the ventricle, which is the blood. Thus, using the endocardium of the heart would undermine the volume difference contributed by the AVPD between ED and ES, just as it would if we used the inner diameter of the telescope. With myocardial thickening secondary to the AV-plane being pulled towards the apex, the longitudinal function contributes to radial fractional shortening in the short axis plane, and would do so even without any radial contraction (100).

3.3.2 Radial contribution to stroke volume

Radial contribution to stroke volume (SV) was further divided into contribution of the lateral walls of each ventricle to SV and of the ventricular septum to either left or right ventricular SV. Septal contribution to SV was quantified in the short axis images as shown in Figure 3.2. The ventricular septum was defined by the LV epicardial border and the RV insertion points that mark the junction between the LV epicardium and the RV epicardium; anteriorly at the junction of the anterior and anteroseptal segments and inferiorly at the junction of the inferior and inferoseptal segments of the LV. The epicardial contours of the LV in ED were copied to the corresponding images in ES in all slices from the base to the apex. This generated an area (diagonal lines in Figure 3.2) that represents the volume contributed to SV by the septal movement. Septal motion towards the LV was denoted a positive contribution to the LVSV. Septal motion towards the RV was denoted a negative contribution to the LVSV or conversely, a positive contribution to RVSV. Lateral contribution to SV was calculated by copying the epicardial contours of the LV in ED to the ES images in all slices from the apex to the base as described above. The area demarcated by the lateral LV epicardial contours in ED and ES and the RV insertion points represents the volume contributed by the lateral displacement of the LV to LVSV. The same was done for the RV using the two RV insertion points and epicardial contours of the RV in ED and ES to calculate the volume contributed by the lateral displacement of the RV to RVSV (Figure 3.2). Basally we only included the slices where both ventricles and the ventricular septum were detected in both ED and ES to avoid including longitudinal displacement in the calculation of septal and lateral contribution to SV.

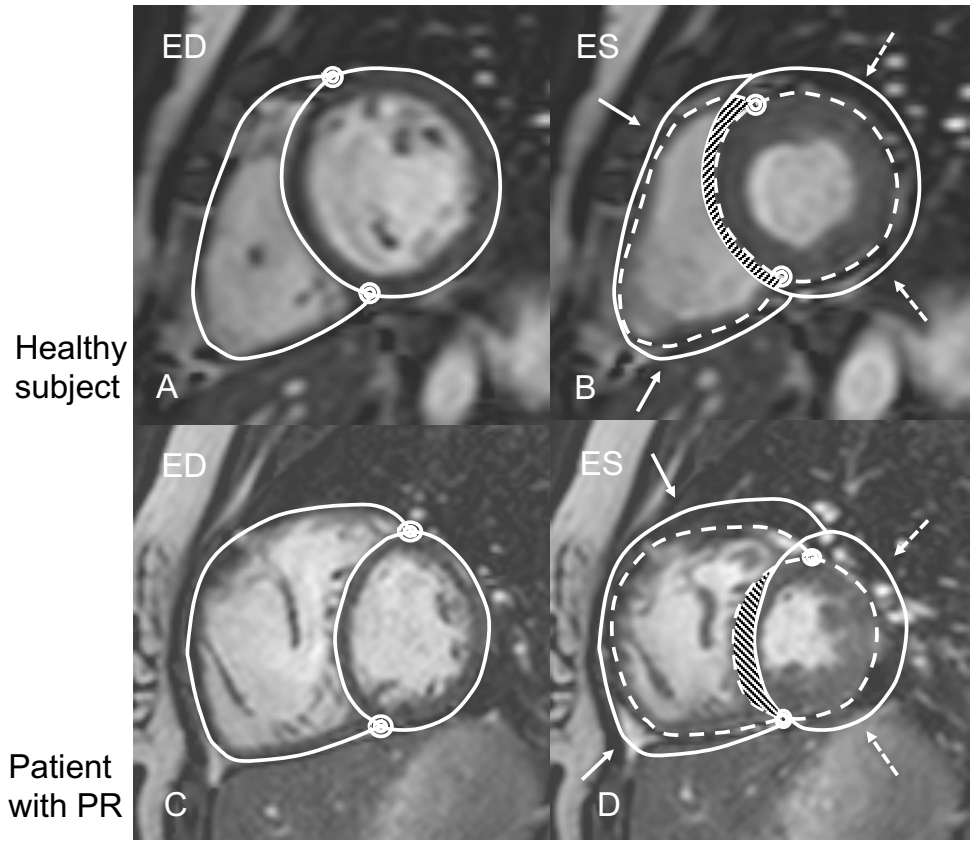

Figure 3.2
Short axis view in end-diastole (ED) and end-systole (ES) in a healthy individual (top row) and a patient with severe pulmonary regurgitation (PR) secondary to tetralogy of Fallot (bottom row). The solid line represents the ED epicardial contour of the left (LV) and right ventricles (RV) and the broken line the ES epicardial contour. The 2 small double circles signify the RV insertion points of the ventricular septum. The diastolic contour is copied to the systolic image to show how the septum moves toward the LV in systole in a healthy individual but to the RV in a patient with PR. The area demarcated by the ED and ES epicardial contours and the RV insertion points (diagonal lines) represents the volume contributed by the septal motion to the stroke volume (SV); a positive contribution to the LVSV in the healthy individual and a negative contribution to the LVSV in the patient with PR. This measurement was done in all short-axis slices from the base to the apex of the heart. In the same manner the contribution of the lateral wall displacement to LVSV (dotted arrows) and RVSV (solid arrows) was calculated by using the two RV insertion points and the lateral epicardial contours of the LV and the RV respectively.

3.3.3 Center of volume and total heart volume variation

The center of volume (COV) of the heart was calculated using the delineation of total heart volume variation (THVV). This was performed by delineation of the pericardial border in short-axis images covering the whole heart (12, 14). All structures within the pericardium were included, ventricles, atria and the intrapericardial parts of the aorta and the pulmonary artery. The total heart volume was obtained in ED and ES by summation of all slices and THVV in percent was calculated as the difference between THV in ED and ES divided by THV at ED. The movement of the center of volume in three anatomical directions, septal-lateral, anterior-inferior, and apical-basal, between ED and ES was calculated to obtain center of volume variation (COVV) (14). A positive septal-lateral value denotes movement of the COV toward septum in systole, a positive anterior-inferior value denotes movement anteriorly in systole, and a positive apical-basal value denotes movement apically in systole.

3.3.4 Statistical analysis

Statistical analysis was performed using Graphpad Prism (v 5.0 in study I, v 6.0 in study II and v 7.0 in study III and IV). Continuous variables were presented as mean ± standard error of the mean (SEM) in studies I and II and as mean ± standard deviation (SD) in studies III and IV. Pearson's correlation was used to examine the relationship between variables. Mann-Whitney and Wilcoxon test were used to test if variables differed between the groups. Results with a P-value of < 0.05 were considered statistically significant. Chi-square test was used in study III to test if New York Heart Association (NYHA) functional class and the dichotomous variables of gender differed between groups. Inter-observer variability was calculated as bias ± SD according to Bland-Altman (57) in nine ASD patients and six healthy controls for LVSV, RVSV, LVAVPD and RVAVPD at rest and during dobutamine stress.

4. Results and comments

4.1 Ventricular pumping in right ventricular volume load

Studies I and III

The role of the ventricular septum was first described using M-mode ultrasonography in 1969 by Popp et al (74) and by Diamond et al in 1971 who described the systolic anterior motion of the septum in patients with atrial septal defect (21). With the development of ultrasound and later MRI for diagnosing congenital heart defects, more studies on septal motion in patients with RV volume and pressure load have followed (23, 44, 63, 77, 80, 105). However, quantification of stroke volume derived from septal motion has not been examined. Study I was designed to calculate the contribution of septal motion to stroke volume in TOF patients with PR and paradoxical septal motion, and to determine a reference value in healthy controls using MRI. With this method, the lateral contribution to SV of both left and right ventricle was also determined. In healthy subjects the septum contributed to LVSV by 7% (range 0-16%) and in patients with PR and RV volume load the septum contributed to RVSV by 8% (range 0-22%, $P<0.001$ compared to healthy controls) (Figure 4.1). In healthy subjects the contribution of the LV lateral wall to LVSV was 36% (range 20-53%) and of the RV lateral wall to RVSV 31% (range 19-46%). In patients with PR the lateral wall contributed to LVSV by 62% (range 38-85%) and to RVSV by 40% (range 25-52%) (Figure 4.2). The longitudinal contribution to stroke volume, calculated from the atrioventricular plane displacement, was determined using a previously validated method (15, 16).

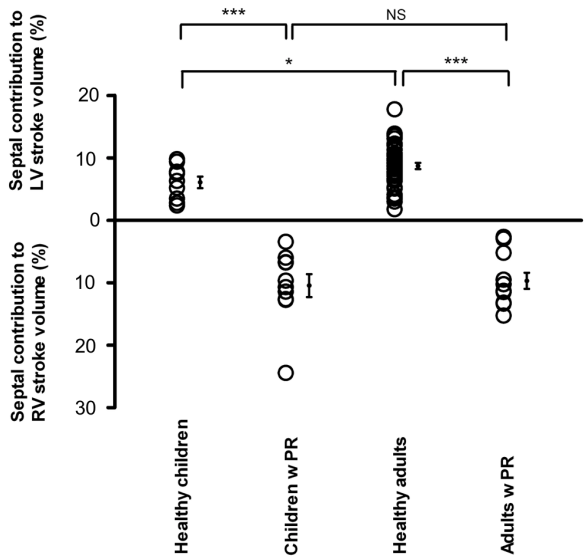

Figure 4.1
Contribution of the ventricular septal movement to LVSV in healthy adults and children and to right RV systolic SV in adults and children with PR. *P < 0.05, **P < 0.01, ***P < 0.001.

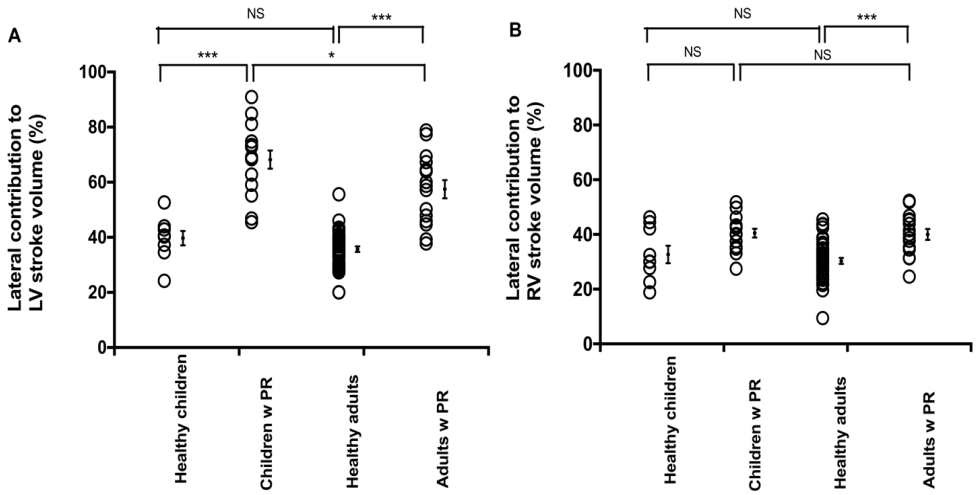

Figure 4.2
Lateral contribution to LVSV (A) and RVSV (B) in healthy adults and children and adults and children with PR. *P < 0.05, ***P < 0.001

In healthy subjects, longitudinal contribution was 59% (range 43-82%) for LVSV and 79% for RVSV (range 60-100%) and in PR patients 54% (range 28%-79%) for LVSV and 47% (range 28-75%) for RVSV (Figure 4.3). The regional contribution to SV in patients with ASD and RV volume load in study III differed from the PR patients (Table 1). ASD patients had preserved longitudinal contribution to SV for both LV and RV and lateral contribution to RVSV. The septum in ASD patients moved paradoxically in 9 out of 16 patients and contributed to RVSV instead of LVSV, leading to a compensatory increase in the lateral contribution to LVSV. Thus, longitudinal contribution to SV was decreased in PR patients but not in ASD patients where longitudinal function was preserved (Figure 4.4).

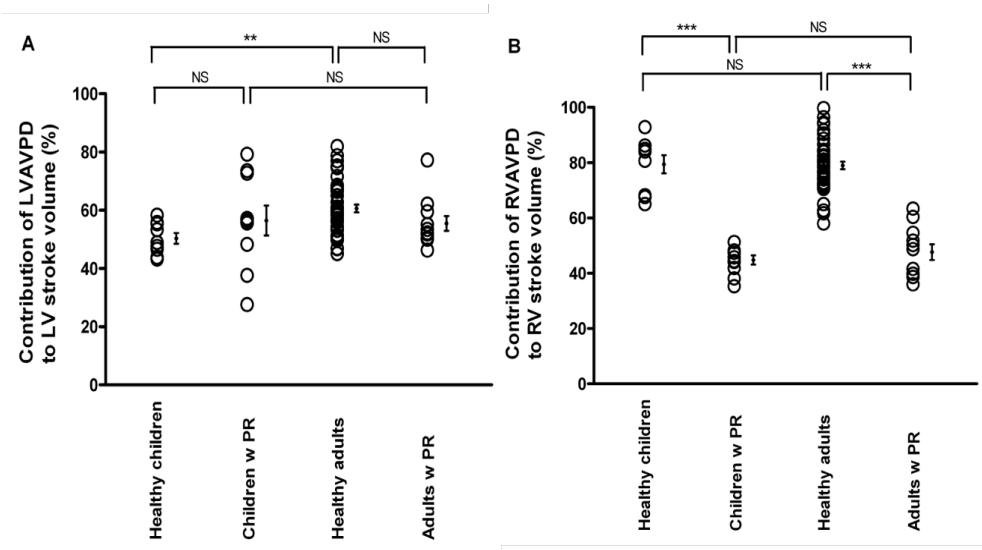

Figure 4.3 Contribution of the AVPD to LVSV (A) and RVSV (B) in healthy adults and children and adults and children with PR. **P < 0.01, ***P < 0.001.

Table 1

Comparision of left and right ventricuarl AVPD and longitudinal (long), lateral (lat) and septal contribution to SV in ASD patients, healthy subjects and PR patients. π P<0.05, when comparing ASD patients and controls, §§ P<0.01, §§§ P<0.001 when comparing PR patients and controls, * P<0.05, *** P<0.001 when comparing PR patients and ASD patients

	ASD patients (n=17)	Healthy subjects (n=10)	PR patients (n=30)
LVAVPD (mm)	16±3 ***	16±2	12±2 §§§
RVAVPD (mm)	22±4 ***	20±4	12±3 §§§
LV long (%)	63±11 *	62±8	54±11 §§
LV lat (%)	40±11 ***	30±8 π	63±14 §§§
Septum (%) (contribution to LVSV)	-1±13 ***	7±4 π	-12±8 §§§
RV long (%)	74±15 ***	79±9	47±10 §§§
RV lat (%)	31±7 ***	30±7	40±7 §§

There was no correlation between RVEDVI and longitudinal contribution to RVSV in either group. Thus, RV size per se does not determine the longitudinal function of the RV. Rather, the etiology for the RV dilation determines the decreased longitudinal contribution to RVSV in PR patients. In figure 4.5 the differences in radial and longitudinal pumping between a healthy subject and a patient with PR are explained. In the healthy subject, where RVSV is equal to LVSV, the longitudinal contribution to RVSV is 80%. In systole, the longitudinal displacement of the AV plane towards the apex evokes subsequent atrial filling of equal volume, i.e., 80% of the RVSV (88). In a patient with moderate PR a large part of the RVSV is derived from the pulmonary regurgitation, to which the AVPD is not coupled. Preserved longitudinal contribution of 80% of RVSV in these patients would result in a systolic inflow to the right atrium larger than the effective SV (RVSV-PR). This

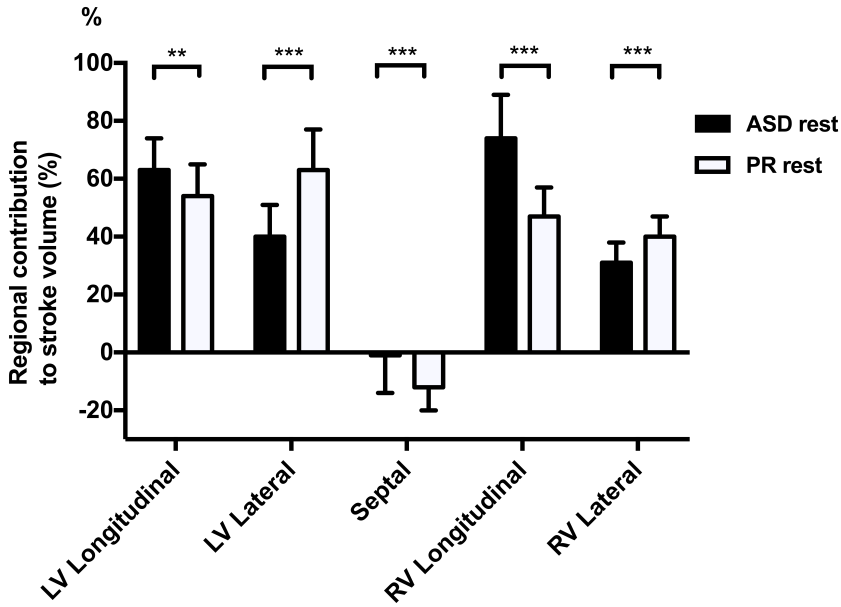

Figure 4.4
Comparison of regional contributors to left (LV) and right ventricular (RV) stroke volume (SV) in patients with ASD (black columns, n=17) and patients with PR (white columns, n=30). Patients with ASD had higher longitudinal contribution to both LVSV and RVSV compared to patients with PR. Conversely, lateral contribution to SV was higher in patients with PR. Net septal contribution to SV was zero in ASD-patients but the septum contributed to RVSV in PR patients. **P<0.01, ***P<0.001.

theoretical example would in turn result in a volume expanded right atrium and a pendulum volume of blood between the right atrium and the caval veins. This is prohibited by decreased longitudinal contribution to RVSV that is compensated for by increased outer volume changes. In contrast to PR patients, the entire RVSV in ASD patients enters the ventricle through the tricuspid valve and therefore the AVPD and atrial filling are physiologically coupled just as in healthy subjects (S. Stephensen et al. 2014). The application of transannular plane systolic excursion (TAPSE), frequently used in echocardiographic evaluation of RV function (78), should therefore be used with caution in patients with PR and RV volume load, since decreased TAPSE in these patients may be a sign of physiological adaptation to abnormal loading condition rather than of RV failure.

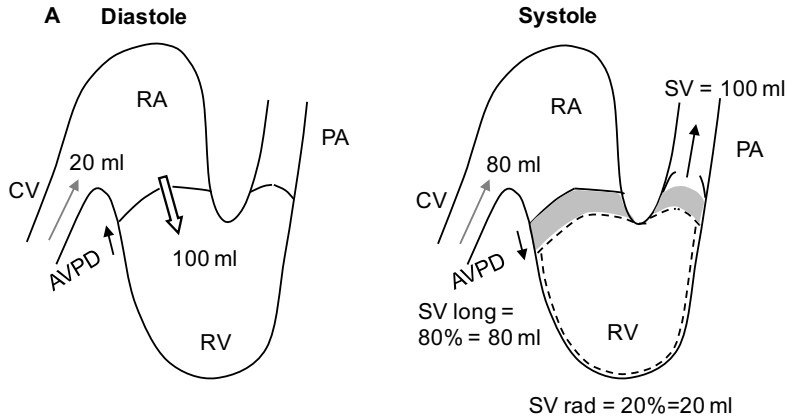

Right atrium and right ventricle in a healthy subject

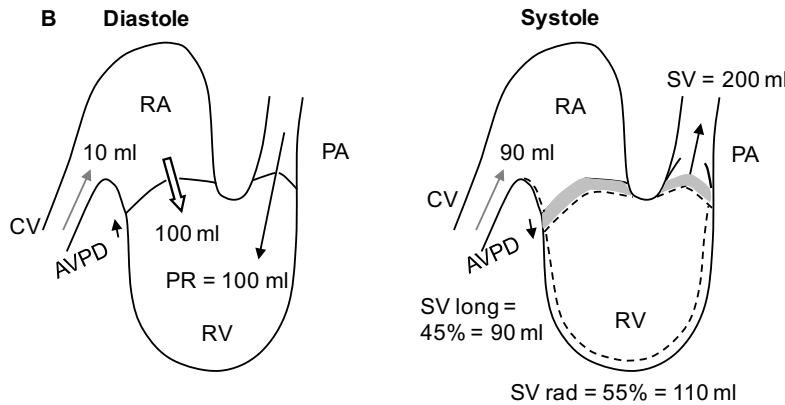

Right atrium and right ventricle in a patient with right ventricular volume overload due to pulmonary regurgitation

Figure 4.5
Schematic long-axis illustration of the inflow and the outflow of the RV, explaining the relationship between longitudinal and radial function in a normal RV and a volume overloaded RV secondary to PR. The outer contour of the heart is shown as a solid line in diastole and as a dotted line in systole. In diastole the AVPD is towards the base of the heart, the blood flows from the RA to the RV (open arrow) and simultaneously blood enters the RA from the caval veins (CV, grey arrow). In systole the AVPD is towards the apex, the RVSV is shown at the pulmonary artery (PA) and simultaneously blood enters the RA from the (CV). The numbers shown in percent represent the longitudinal (SV long) and radial (SV rad) contribution to SV. A: RA and RV in a normal subject. Net inflow from the caval veins to the RA is 100 ml; 20 ml in diastole and 80 ml in systole. In diastole 100 ml of blood are drawn in from the RA to the RV. SV is 100 ml where 80% or 80 ml is generated by the AVPD (SV long) and 20% or 20 ml is generated by the radial displacement (SV rad). B: RA and RV of a patient with PR of 100 ml, dilated RV and longitudinal and radial function as we have observed in the study. In diastole 100 ml of blood are drawn in from the RA to the RV but at the same time there is a PR of 100 ml from the PA to the RV. The SV is thus twice as big as in the normal subject or 200 ml. The radial contribution (SV rad) is larger, contributing to 55% of the SV or 110 ml. The AVPD (SV long) is decreased, only contributing to 45% or 90 ml of the SV. This prompts the same amount of 90 ml to be drawn in from the caval veins to the RA in systole and 10 ml in diastole.

When interpreting longitudinal and radial contribution to SV it is important to distinguish between the shortening of individual myofibers and the net outcome of myocardial shortening. Measurements of regional strain with velocity-encoded MRI and echocardiography speckle tracking are often used to assess myocardial function. LV global longitudinal strain in healthy subjects measured with MR was 18% (40) and in a study on patients with TOF (54) longitudinal strain was 15% in the LV and 18% in the RV free wall. These findings should not be mixed with the longitudinal contribution to SV which is the product of AVPD and the epicardial short axis area. Rather, the complex arrangement of helical and circular myocardial fibers that shorten in a three-dimensional mesh will combine in a net result of longitudinal shortening that provides 60% of the SV in a healthy LV and 80% in a healthy RV. Individual myocytic shortening is only 15% and leads to only 8% increase in myocyte diameter, but the net outcome is LV radial wall thickening of 40% and ejection fraction of 60% (18, 82, 87, 100). Therefore, regional measurements of, e.g., longitudinal strain cannot be used directly to explain the longitudinal contribution to SV, which is the net global outcome of said regional myocardial shortening.

4.2 Pulmonary regurgitation

Study I

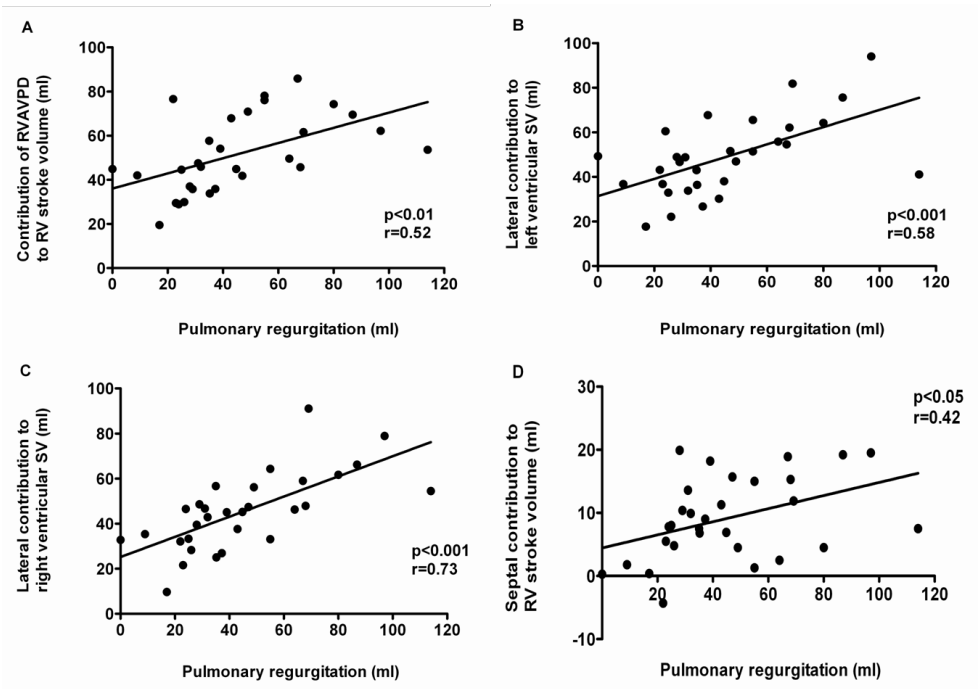

Figure 4.6
Correlation between PR and (A) contribution of RVAVPD to SV, (B) contribution of lateral displacement to LVSV, (C) contribution of lateral displacement to RVSV and (D) contribution of septal movement to RVSV.

The pulmonary regurgitation seems to play a central role in the altered pumping mechanics seen in patients with RV volume load due to PR. We found correlation between the volume of PR and the volume contributed to SV by the lateral walls of the LV and the RV and the volume contributed to RVSV by the AV-plane and the septum (Figure 4.6). It is possible that the RV volume overload and the regurgitation volume from the pulmonary artery, lead to stretching of myofibers with subsequent distorted meshwork, a more spherical architecture, and overexpansion of the RV. These structural changes would alter the contraction pattern to a greater radial contribution, thereby limiting the movement of the AV plane in diastole and conversely decrease the inflow of blood to the RA in systole as explained in Figure 4.5. Alterations in myocardial architecture have been described by Pettersen et al in patients with a systemic RV (71). They studied myocardial strain by CMR tagging

in Senning-operated patients with transposition of the great arteries. In these patients, where the RV serves as the systemic ventricle, the shortening pattern changed toward that of the LV, with predominant circumferential and less longitudinal contraction.

4.3 Center of volume variation

Study I

An important difference between the cohort of TOF patients in study I and both healthy controls and ASD patients in study III is the fact that all the TOF patients have had sternotomy and an open-heart surgery with cardiopulmonary bypass and some patients have undergone reoperation with pulmonary valve replacement. This does not only influence myocardial function (63) but can also cause retrosternal adhesions of the pericardium, potentially affecting the movement of the heart. In such a scenario, septal movement would be that of a passive bulk motion, instead of active contraction. To determine if this was the case we measured systolic wall thickening but found no differences between the septum and the LV lateral wall in patients with PR. Furthermore, measurement of the center of volume variation (COVV) between diastole and systole showed that COVV in the septal and anterior direction was similar in patients compared to healthy subjects. The inward movement of the RV anterior, lateral, and diaphragmal walls was preserved in children and increased in adult patients with PR compared to healthy subjects, making pericardial adhesions unlikely. Riesenkampf et al found decreased RA reservoir function and abnormal RA filling in TOF patients. They concluded that this finding was a direct effect of cardiac surgery and myocardial scarring since these findings were not present in patients with isolated PR and without prior surgery (76). However, support for the notion that PR per se is a source of decreased longitudinal function was seen in a recent study by Kopic et al on piglets with PR without confounding factors of previous surgery (49). PR was created in piglets by transcutaneously inserting a stent in the pulmonary valve annulus. The following months, the regional cardiac function changed towards decreased longitudinal and increased radial function as seen in our study on TOF patients. Two and three months after the creation of PR the piglets underwent transcutaneous PVR and a month later these parameters of regional pumping had almost normalized again. This study also found a strong correlation between RV longitudinal function and pulmonary capillary wedge pressure which might emphasize the importance of RV function for the filling of the LV (49).

4.4 Dobutamine-atropine stress testing and ventricular function

Study II-IV

ASD patients and controls responded in a similar manner to dobutamine stress. In both groups, longitudinal contributions to LVSV and RVSV were lower and lateral contributions higher during stress. There was a mismatch in in- and outflow from the heart and a deviation from the near constant volume of the pericardial sac, presenting as increased total heart volume variation during dobutamine stress in both ASD patients and controls (91). The results are in line with our previous findings in healthy volunteers during supine exercise (89). Ventricular volumes in healthy subjects were comparable to a recent exercise CMR study by La Gerche et al where LVEDV was unchanged between rest and stress but decreased LVESV led to increased SV at stress (30). The max heart rate and CO during exercise in this study were considerably higher than in our study (164±10 bpm and 25.4±4.5 L/min in athletes and 152±27 bpm and 21.6±5.7 L/min in arrhythmia patients). A small but insignificant decrease in ED volumes was observed during dobutamine stress which was not noted during physical stress. This might be related to the lack of muscle pumping in the lower extremities which facilitates venous return during physical exercise but is absent in medically induced stress. Our conclusion is that dobutamine-atropine, despite limitations, can be used as a substitute for exercise when assessing cardiac function during stress.

4.5 Hemodynamic changes during dobutamine-atropine stress

Study II

Heart rate increased in patients (76% increase) and healthy subjects (94%) during dobutamine stress. In patients, left ventricular stroke volume (LVSV) had a non-significant increase of 7% during stress, and RV stroke volume (RVSV) had a non-significant decrease of 6%, leading to a decreased shunting volume per heartbeat by 28% during stress ($P<0.001$), Table 2. This resulted in an increase in systemic CO during stress by 90+11% and in pulmonary CO by 43+7% compared with rest ($P<0.001$ for both) (Figure 4.7).

Table 2
Comparison of absolute and relative systemic and pulmonary blood flow in ASD patients at rest and during dobutamine stress. *** P<0.001

	ASD rest (n=20)	ASD dobutamine (n=20)
HR (bpm)	71±3	122±3 ***
Systemic CI (L/min/m^2)	2.9±0.1	5.4±0.3 ***
Pulmonary CI (L/min/m^2)	5.7±0.5	7.9±0.5 ***
QP/QS	2.0±0.2	1.5±0.1 ***
Absolute shunt volume (L/min)	5.1±0.8	4.5±1.0
Shunt per heartbeat (mL)	70±9	38±9 ***

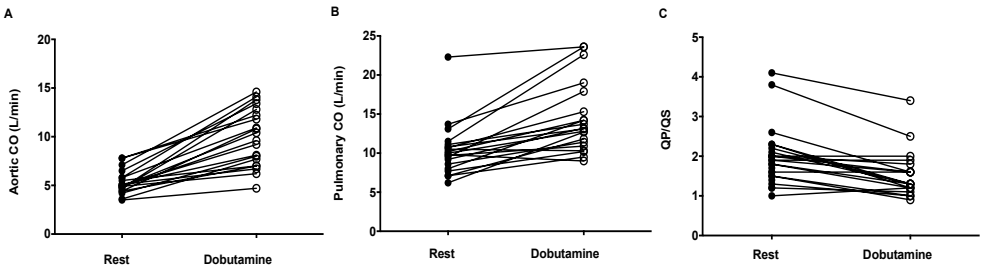

Figure 4.7
Aortic cardiac output (A), pulmonary cardiac output (B), and pulmonary to systemic flow ratio (QP/QS) (C) at rest and during dobutamine stress in 20 patients with ASD.

Thus, the pulmonary to systemic flow ratio (QP/QS) was lower during stress (1.5+0.1) compared with rest (2.0+0.2, P<0.001). However, there was no difference in the mean absolute left-to-right shunt per minute between rest and stress (5.1+0.8 vs. 4.5+1.0 L/min, P = 0.32). Mean ASD diameter was 15.3+1.3 mm and mean cross-sectional area indexed to BSA was 1.0+0.2 cm^2/m^2. The latter did neither correlate to absolute shunt flow (L/min/BSA) at rest (r = 0.47, P = 0.07) nor during dobutamine stress (r = 0.44, P = 0.09), Figure 4.8 A. However, ASD size correlated to QP/QS and shunting volume per heartbeat (mL/BSA) at rest (r = 0.75, P < 0.001 and r = 0.70, P < 0.01, respectively) and during dobutamine stress (r = 0.50, P < 0.05 and r = 0.60, P < 0.05, respectively), Figure 4.8 B and C. Also, there was an inverse correlation between indexed ASD size and systemic CI at rest (r = 20.50, P < 0.05). During dobutamine stress, left-to-right shunting volume decreased, which resulted in more balanced stroke volumes in the left and right ventricle, and a larger increase in systemic compared to pulmonary cardiac index. Thus, during dobutamine stress, there was a greater increase in trans-mitral flow compared to trans-septal flow and the ASD size had less impact on left-to-right shunting. A few possible explanations for the decrease in shunting fraction will be discussed.

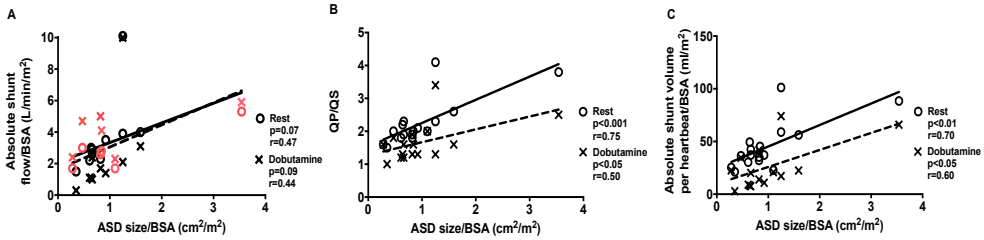

Figure 4.8 Linear regression analysis between the cross-*sectional* area of the ASD indexed to body surface area (BSA), and (A) absolute shunt flow indexed to BSA at rest (open circles) and during dobutamine stress (crosses), (B) pulmonary to systemic flow ratio (QP/QS) at rest (open circles) and during dobutamine stress (crosses), and (C) shunt volume per heartbeat indexed to BSA at rest (open circles) and during dobutamine stress (crosses) in 16 ASD patients. QP/QS was strongly related to indexed ASD size at rest (Y ¼ 0.70X + 1.55) and to a lesser degree during dobutamine stress (Y ¼ 0.39X + 1.28). QP/QS decreased during dobutamine stress for all ASD sizes. Black colour in Figure 4A represents patients with decreased shunt flow during stress and red colour represents patients with increased shunt volume during stress.

First, the ASD might become more restrictive with increased flow, limiting the left-to-right shunt. The correlation coefficients between ASD size and QP/QS at rest varies (24, 27, 73) and studies during stress are lacking. Our study showed decreased QP/QS in all patients at stress, independent of ASD size. Second, conditions that either increase LV compliance or reduce RV compliance would cause decreased shunting through ASD. The left-to-right shunting occurs predominantly in late systole, early diastole and during atrial contraction (52). In healthy subjects, the pulmonary capillary wedge pressure, representing LAP, increases with exercise (97) and LV end-diastolic pressure increases or is unchanged between rest and supine exercise (66). However, the nadir of diastolic pressure is lower during exercise than at rest due to enhanced LV relaxation and elastic recoil. This leads to increased atrioventricular pressure gradient and enhanced flow across the mitral valve during exercise (66). With advanced age mild to moderate pulmonary hypertension can develop (34). La Gerhe et al have studied the difference between vascular resistance and afterload pressure in the systemic versus pulmonary vasculature at rest and during exercise based on Poiseuille's law (Pressure = Resistance x Flow) (31, 32). At rest the pulmonary vascular resistance is very low and has limited capacity for further reduction during exercise. The systemic vascular resistance, on the other hand is high and drops significantly with exercise. Thus, exercise-induced increase in blood flow and limited ability to adjust pulmonary vascular resistance leads to greater rise in RV afterload pressure than in the LV. Exercise therefore results in proportionally higher workload on the RV which could limit the RV cardiac output (31, 32). This has also been suggested in a study on patients with open and closed ASD (9). Therefore, in ASD patients with chronically increased pulmonary blood flow and elevated pulmonary artery pressure causing RV hypertrophy, exercise might cause even higher work load on the RV with decreased compliance and

elevated right atrial pressure, limiting the shunt across the ASD. Third, the bulging of the ventricular septum to the left affects LV compliance through diastolic ventricular interdependence (64). During dobutamine stress the mean septum contribution to SV was zero meaning that the leftward bulging during diastole decreased. This might improve the LV filling during stress in ASD patients and reduce the shunt. Lastly, decreased shunt during stress might be related to atrial kinetic energy that contributes to ventricular filling via inertia of the rotating blood generated by systolic contraction and the position of the veins (2). The kinetic energy plays a larger part in heart pumping during stress (13) and may contribute to increased transmitral flow during stress in ASD patients.

4.6 Effect of ASD closure on ventricular volumes and cardiac pumping; short- and long-term follow-up

Study III and IV

Closure of the ASD resulted in a decrease in RVSV by 27±20% ($P=0.001$), increase in longitudinal contribution to RVSV ($P<0.05$) and a decrease in longitudinal contribution to LVSV ($P<0.01$) compared to before closure. Septal movement during systole shifted from right to left and contributed to LVSV the day after closure, instead of RVSV pre-intervention ($P<0.001$) (Figure 4.9). The reverse remodeling process with increased LVEDV and decreased RVEDV had begun the day after ASD closure, which is in concordance with previous studies (98). The pumping mechanisms in patients with RV overload due to left-to-right shunting thus adjust when the stroke volumes equalize, which may be driven by the changing movement of the ventricular septum during the heart cycle. The explanation for the decreased LV longitudinal pumping after ASD closure might also be an effect of LV diastolic dysfunction that becomes unmasked with the increased LV preload after ASD closure (20, 84). Apart from RV volume load, LV pressure likely affects

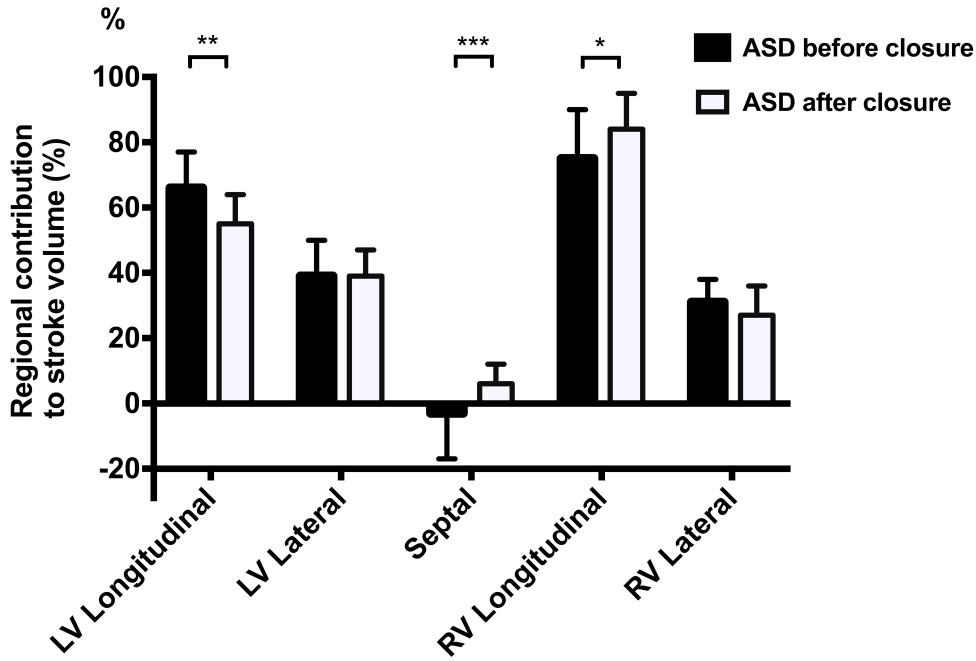

Figure 4.9
Comparison of regional contributors to left (LV) and right ventricular (RV) stroke volume in patients with ASD before (black columns) and after (white columns) transcutaneous closure of the ASD. Closure of the ASD caused a decrease in longitudinal contribution to LVSV and in contrast an increased longitudinal contribution to RVSV. The septum changed from contributing to RVSV before closure to contributing to LVSV after closure of the ASD. *P < 0.05, **P < 0.01, ***P < 0.001.

the septal contour in ASD patients. The effect of increased LV preload, with ASD closure, on LV end-diastolic pressure (EDP) is thought to be age dependent, where a larger increase in LVEDP can be expected in older patients, with decreased myocardial relaxation and compliance (37). We did not have invasive pressure data immediately after ASD closure and with a wide age range in the patient group (27-81 years) it is difficult to interpret the effect of LV pressure on radial and longitudinal motion in this study.

The changes in left and right ventricular volumes and stroke volumes following ASD closure are shown in figure 4.10 and 4.11.

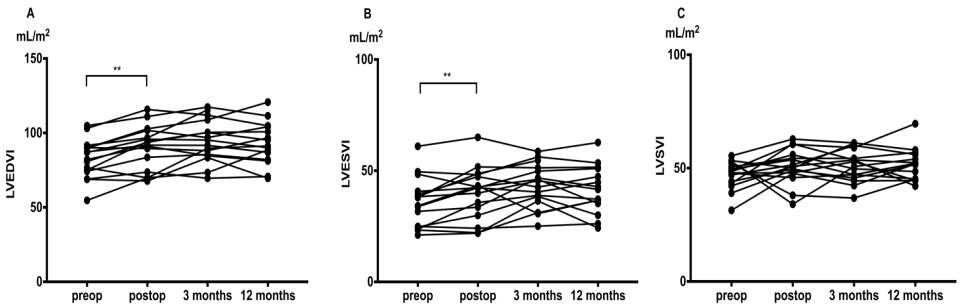

Figure 4.10
Left ventricular ED and ES volumes and SV indexed to BSA before and the day after ASD closure and at 3 and 12 months follow-up, **P < 0.01.

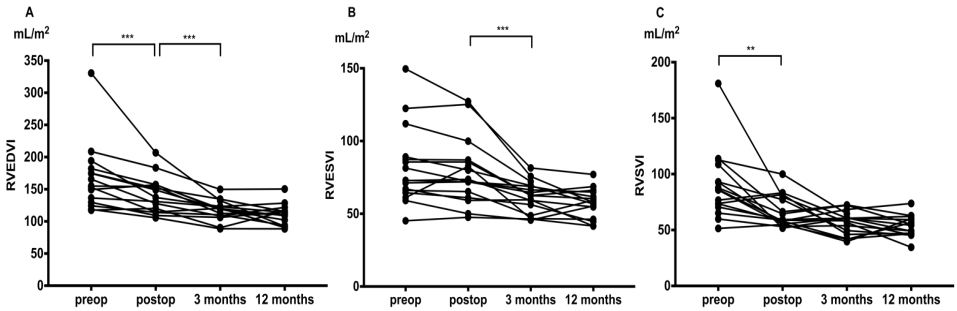

Figure 4.11
Right ventricular ED and ES volumes and SV indexed to BSA before and the day after ASD closure and at 3 and 12 months follow-up, **P < 0.01, ***P < 0.001.

At 12 months follow-up RV volumes were still larger than LV volumes (P<0.001 for both EDVI and ESVI) but SV did not differ (P=0.39). Our results on RV adaptation to decreased volume load are in concordance with other studies on ASD-patients (70, 85, 98). However, we did not find any increase in LVEF after ASD closure as documented in other studies, and proposed to be related to improved exercise capacity (35).

4.7 Ergospirometry results and relation to dobutamine-atropine stress

Study II and IV

We did not find improvement in aerobic capacity when comparing absolute values of VO_2 *peak* before ASD closure and at 12 months follow-up (P=0.07). However, when comparing VO_2 *peak* as percentage of predicted value the aerobic capacity had improved at 12 months follow-up (P<0.01) (Table 3). This may be related to the age of the patient group at ASD closure (52±17 years). Age is an influential factor in the Hansen/Wasserman equation used for calculation of predicted VO_2 *peak* (104). Previous studies exerciseon aerobic capacity of patients with ASD often show significantly impaired VO_2 *peak* or VO_2 *peak %* of predicted values (8, 25, 35, 41, 96). In these studies, VO_2 *peak* was reported between 13.1 and 23.5 mL/min/kg and VO_2 *peak %* of predicted values ranging from 50 to 91%. The patients in our study had peak oxygen consumption of 26.7 mL/min/kg or 101% of predicted value for healthy subjects, which implies that the patients in our study were relatively fit compared to other studies (36, 48, 95, 96). Patients with impaired exercise capacity preoperatively may have a larger capacity for improvement compared to patients that already have normal VO_2 *peak*. Previous studies have

Table 3.
Aerobic capacity (VO_2) in patients with ASD before and 12 months after closure and in healthy controls. NYHA; New Yorks Heart Association, ** P<0.01, *** P<0.001, when comparing ASD patients and healthy subjects, ++ P<0.01 when comparing ASD patients before and after closure.

	ASD preop	ASD 12 months f/u	Healthy subjects
VO_2 *peak* (mL/min/kg)	26±7 ***	28±8 ***	45±8
VO_2 *peak %*	101±19 ***	108±19 **, ++	138±25
NYHA class	I=6 (38%), II=7 (43%), III=3 (19%)		I=13 (87%), II=2 (13%)

shown conflicting results after closure of ASD with both improved and impaired exercise capacity (36, 48, 83). A possible reason for the lack of improvement is adaptation to a certain degree of limitation. The interests and daily activity of ASD patients may be a consequence of unknown heart condition and undergoing treatment of the heart defect is not expected to change their lifestyle or interests overnight. It may take even longer than 12 months to appreciate being able to perform the physical activity made possible by such a treatment.

A study by Kröönström et al. found decreased isotonic muscle function in adults with congenital heart defects compared to healthy subjects (50). This was thought to be a marker for a generally inactive physical lifestyle in these patients. Studies have described increased LV end-diastolic pressure following ASD closure in the older population, where abnormal LV relaxation, increased LV stiffening and impaired contraction due to chronic underload may exist (22, 58, 59). Left atrial (LA) pressure before ASD closure in our study (7±3 mm Hg) was not increased and we do not have pressure data from the LA or LV after ASD closure. However, diastolic dysfunction, that becomes unmasked with ASD closure, could be a factor explaining the modest improvement in exercise capacity. In a recent study comparing patients with improved vs non-improved VO2 peak one month after ASD closure, the non-improved group had decreased LV torsion, increased longitudinal global RV strain and increased level of pro-BNP after ASD closure (45). This was considered a sign of early LV dysfunction and delayed RV remodeling after ASD closure. However, whether these results have a long-term prognostic value or if the parameters improve with time is not known.

There was a moderate negative correlation (r=-0.56) between QP/QS or shunt per heart beat indexed to BSA at rest and improvement in VO_2% at 12 months follow-up but this correlation was not found during dobutamine stress (Figure 4.12). Thus, patients who had the largest improvement in VO_2 *peak %* were those with smaller shunt at rest before ASD closure, but in patients with larger shunts the improvement was not as profound. A prior study by Kobayashi et al. showed that in patients with large shunts, the high pulmonary blood flow can cause irreversible damage to pulmonary arterioles leading to increased pulmonary vascular resistance (46). This explanation is less likely in our cohort since pulmonary artery pressure, measured before ASD closure, was within normal limits (19±5 mm Hg). There was a moderate

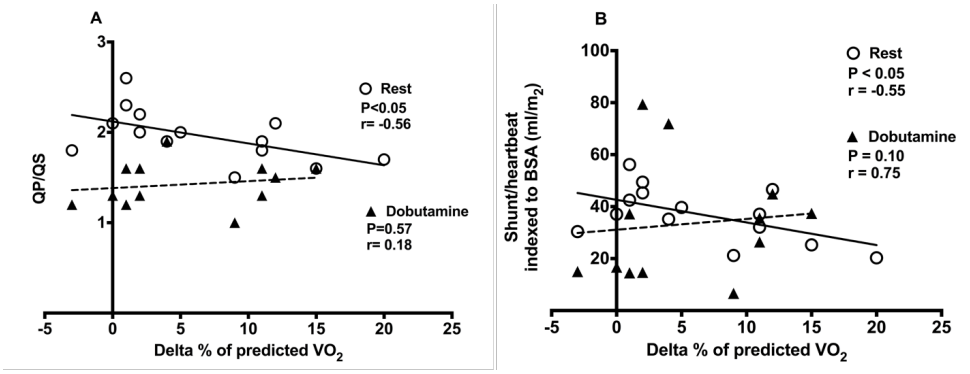

Figure 4.12
Linear regression analysis between the improvement in VO_2 *peak* presented as percentage of predicted value and pulmonary-to-systemic flow ratio (QP/QS) (A) and shunt per heart beat indexed to body surface area (BSA) (B) at rest (open circles, solid line) and during dobutamine stress (triangles, broken line) before ASD closure.

correlation between VO_2 *peak* and systemic and pulmonary CO during dobutamine stress in controls (Figure 4.13 A) but only with aortic CO ($r = 0.77$, $P < 0.001$) in ASD patients (Figure 4.13 B). This is probably explained by the fact that the body is dependent on a high systemic outflow to perform exercise. Whether this happens during a high or low degree of shunting does not seem to be relevant to the exercising body, as long as systemic CO is delivered at an appropriate rate. There was an inverse correlation between VO_2 *peak* and QP/QS at rest ($r = 20.48$, $P < 0.05$) but not during dobutamine stress in ASD patients ($r = 20.39$, $P = 0.09$) (Figure 4.13 C). Exercise capacity was not significantly related to left-to-right shunting, pulmonary blood flow or RV volumes during stress.

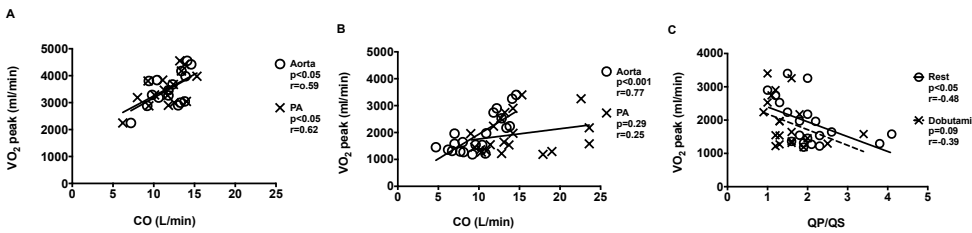

Figure 4.13
Linear regression analysis between systemic (Aorta, open circles) or pulmonary (PA, crosses) cardiac output during dobutamine stress in (A) healthy controls and (B) patients with ASD and VO_2 peak. Systemic cardiac output during dobutamine stress was related to exercise capacity in patients (Aorta; y ¼ 183.1x + 107.9) whereas pulmonary cardiac output was not. Figure C: Linear regression analysis showed an inverse correlation at rest (open circles) between QP/QS and VO_2 peak but not during dobutamine stress (crosses).

5. Conclusions and future thoughts

This thesis has studied patients with congenital heart defects of different etiology that cause volume loading of the right ventricle and how this condition affects cardiac pumping. It has quantified longitudinal, lateral and septal contribution to stroke volume and explained how the AV-plane movement is coupled to the systolic inflow to the heart and the effective stroke volume. The conclusions of each paper were:

I. Pulmonary regurgitation leads to decreased longitudinal contribution to RVSV, a compensatory increase in lateral contribution to RVSV and paradoxical septal motion that contributes to RVSV instead of LVSV. In healthy subjects the septum contributes to 7% of LVSV

II. In patients with ASD pulmonary-to-systemic flow ratio and left-to-right shunt per heart beat is decreased during stress. High systemic cardiac output during stress is strongly related to exercise capacity in ASD patients.

III. Longitudinal and lateral contribution to SV in patients with ASD and RV volume overload is similar to healthy subjects and differ from patients with RV volume load due to PR. Pumping mechanics thus depend on the etiology for rather than degree of RV size. Changes in pumping mechanics are seen on the day after transcutaneous ASD closure.

IV. Quantification of shunt size or ventricular volumes during stress did not predict exercise capacity 12 months after transcutaneous ASD closure. Patients with smaller QP/QS had larger improvement in predicted exercise capacity at follow-up. Ventricular remodeling after ASD closure is fast on the left side and prolonged on the right side.

Considering that exercise can reveal symptoms caused by heart defects that are asymptomatic at rest, it is important to be able to simulate stress in as physiological way as possible when assessing the hemodynamic effects of the heart defects. Since the project plan for this thesis was laid down progress has been made in CMR stress imaging (30, 89) minimizing movement artifacts during exercise in the scanner. Today the stress CMR would most likely be done during exercise and not medically induced stress. In our follow-up study, we found larger improvement in VO_2 *peak %* in patients with small shunts compared to large shunts. This finding raises the

question if we should be closing atrial septal defects that are generally considered small and of little hemodynamic significance. It would therefore be interesting to close the defect in patients with small ASD included in study II and do a follow-up exercise test 12 months later. If improved it might change our inclusion criteria for ASD closure. The notion that we may be underestimating the significance of "small" shunt defects is supported by two recent studies that showed lower exercise tolerance in patients with asymptomatic ASD (94) and VSD (56) compared to healthy controls.

Recent studies have revealed how pulmonary regurgitation in TOF patients leads to RV remodeling during the first few years after surgery but then reaches more steady state, with slowly progressive RV volumes in the majority of young adults (79). However, in 15% of patients RV deterioration is rapid prompting early pulmonary valve replacement (6). Given the relationship we found between PR and regional contribution to SV, these parameters might be of value in predicting progressive versus non-progressive disease on follow-up CMR studies in TOF patients.

References

1. **Arheden H**, **Holmqvist C**, **Thilen U**, **Hanséus K**, **Björkhem G**, **Pahlm O**, **Laurin S**, **Ståhlberg F**. Left-to-right cardiac shunts: comparison of measurements obtained with MR velocity mapping and with radionuclide angiography. 1999.
2. **Arvidsson PM**, **Töger J**, **Heiberg E**, **Carlsson M**, **Arheden H**. Quantification of left and right atrial kinetic energy using four-dimensional intracardiac magnetic resonance imaging flow measurements. *J Appl Physiol* 114: 1472–81, 2013.
3. **Babu-Narayan S V.**, **Kilner PJ**, **Li W**, **Moon JC**, **Goktekin O**, **Davlouros PA**, **Khan M**, **Ho SY**, **Pennell DJ**, **Gatzoulis MA**. Ventricular fibrosis suggested by cardiovascular magnetic resonance in adults with repaired tetralogy of Fallot and its relationship to adverse markers of clinical outcome. *Circulation* 113: 405–413, 2006.
4. **Bartelds B**, **Borgdorff MA**, **Smit-van Oosten A**, **Takens J**, **Boersma B**, **Nederhoff MG**, **Elzenga NJ**, **van Gilst WH**, **De Windt LJ**, **Berger RMF**. Differential responses of the right ventricle to abnormal loading conditions in mice: pressure vs. volume load. *Eur J Heart Fail* 13: 1275–1282, 2011.
5. **Bellenger NG**, **Grothues F**, **Smith GC**, **Pennell DJ**. Quantification of right and left ventricular function by cardiovascular magnetic resonance. *Herz* 25: 392–9, 2000.
6. **Bhagra CJ**, **Hickey EJ**, **Van De Bruaene A**, **Roche SL**, **Horlick EM**, **Wald RM**. Pulmonary Valve Procedures Late After Repair of Tetralogy of Fallot: Current Perspectives and Contemporary Approaches to Management. *Can J Cardiol* 33: 1138–1149, 2017.
7. **Brochu M-C**, **Baril J-F**, **Dore A**, **Juneau M**, **De Guise P**, **Mercier L-A**. Improvement in Exercise Capacity in Asymptomatic and Mildly Symptomatic Adults After Atrial Septal Defect Percutaneous Closure. *Circulation* 106, 2002.
8. **Brochu MC**, **Baril JF**, **Dore A**, **Juneau M**, **De Guise P**, **Mercier LA**. Improvement in exercise capacity in asymptomatic and mildly symptomatic adults after atrial septal defect percutaneous closure. *Circulation* 106: 1821–1826, 2002.
9. **Van De Bruaene A**, **La Gerche A**, **Prior DL**, **Voigt J-U**, **Delcroix M**, **Budts W**. Pulmonary vascular resistance as assessed by bicycle stress echocardiography in patients with atrial septal defect type secundum. *Circ Cardiovasc Imaging* 4, 2011.
10. **Buechel ER V.**, **Dave HH**, **Kellenberger CJ**, **Dodge-Khatami A**, **Pretre R**, **Berger F**, **Bauersfeld U**. Remodelling of the right ventricle after early pulmonary valve replacement in children with repaired tetralogy of Fallot: assessment by cardiovascular magnetic resonance. *Eur Heart J* 26: 2721–2727, 2005.
11. **Carlsson M**, **Andersson R**, **Bloch K**, **Steding-Ehrenborg K**, **Mosén H**, **Stahlberg F**, **Ekmehag B**, **Arheden H**. Cardiac output and cardiac index measured with

cardiovascular magnetic resonance in healthy subjects, elite athletes and patients with congestive heart failure. *J. Cardiovasc. Magn. Reson.* 14: 51, 2012.

12. **Carlsson M**, **Cain P**, **Holmqvist C**, **Stahlberg F**, **Lundback S**, **Arheden H**. Total heart volume variation throughout the cardiac cycle in humans. *Am J Physiol Heart Circ Physiol* 287: H243-50, 2004.
13. **Carlsson M**, **Heiberg E**, **Toger J**, **Arheden H**. Quantification of left and right ventricular kinetic energy using four-dimensional intracardiac magnetic resonance imaging flow measurements. *AJP Hear. Circ. Physiol.* 302: H893–H900, 2012.
14. **Carlsson M**, **Rosengren A**, **Ugander M**, **Ekelund U**, **Cain P**. Center of volume and total heart volume variation in healthy subjects and patients before and after coronary bypass surgery. *Clin Physiol Funct Imaging* 25: 226–233, 2005.
15. **Carlsson M**, **Ugander M**, **Heiberg E**, **Arheden H**. The quantitative relationship between longitudinal and radial function in left, right, and total heart pumping in humans. *Am J Physiol Heart Circ Physiol* 293: H636–H644, 2007.
16. **Carlsson M**, **Ugander M**, **Mosén H**, **Buhre T**, **Arheden H**. Atrioventricular plane displacement is the major contributor to left ventricular pumping in healthy adults, athletes, and patients with dilated cardiomyopathy. *Am J Physiol Heart Circ Physiol* 292: H1452–H1459, 2007.
17. **Chan AK**, **Govindarajan G**, **Del Rosario ML**, **Aggarwal K**, **Dellsperger KC**, **Chockalingam A**. Dobutamine stress echocardiography Doppler estimation of cardiac diastolic function: a simultaneous catheterization correlation study. *Echocardiography* 28: 442–7, 2011.
18. **Cheng A**, **Nguyen TC**, **Malinowski M**, **Daughters GT**, **Miller DC**, **Ingels NB**. Heterogeneity of left ventricular wall thickening mechanisms. *Circulation* 118: 713–721, 2008.
19. **Coghlan C**, **Hoffman J**. Leonardo da Vinci's flights of the mind must continue: cardiac architecture and the fundamental relation of form and function revisited. *Eur J Cardio-thoracic Surg* 29: 4–17, 2006.
20. **Dexter L**. Atrial septal defect. *Br Heart J* 18: 209–25, 1956.
21. **Diamond M a**, **Dillon JC**, **Haine CL**, **Chang S**, **Feigenbaum H**. Echocardiographic features of atrial septal defect. *Circulation* 43: 129–135, 1971.
22. **Ermis P**, **Franklin W**, **Mulukutla V**, **Parekh D**, **Ing F**. Left Ventricular Hemodynamic Changes and Clinical Outcomes after Transcatheter Atrial Septal Defect Closure in Adults. *Congenit Heart Dis* 10: E48–E53, 2015.
23. **Feneley M**, **Gavaghan T**. Paradoxical and pseudoparadoxical interventricular septal motion in patients with right ventricular volume overload. *Circulation* 74: 230–238, 1986.
24. **Forfar JC**, **Godman MJ**. Functional and anatomical correlates in atrial septal defect. An echocardiographic analysis. *Br Heart J* 54: 193–200, 1985.
25. **Fredriksen PM**, **Veldtman G**, **Hechter S**, **Therrien J**, **Chen A**, **Warsi MA**, **de Koning WB**. Aerobic capacity in adults with various congenital heart diseases. *Am J Cardiol* 87: 310–314, 2001.
26. **Friedberg MK**, **Redington AN**. Right versus left ventricular failure: Differences,

similarities, and interactions. *Circulation* 129: 1033–1044, 2014.

27. **Fuse S**, **Tomita H**, **Hatakeyama K**, **Kubo N**, **Abe N**. Effect of size of a secundum atrial septal defect on shunt volume. *Am J Cardiol* 88: 1447–1450, A9, 2001.

28. **Gatzoulis M a**, **Balaji S**, **Webber S a**, **Siu SC**, **Hokanson JS**, **Poile C**, **Rosenthal M**, **Nakazawa M**, **Moller JH**, **Gillette PC**, **Webb GD**, **Redington a N**. Risk factors for arrhythmia and sudden cardiac death late after repair of tetralogy of Fallot: a multicentre study. *Lancet* 356: 975–981, 2000.

29. **Geleijnse ML**, **Fioretti PM**, **Roelandt JR**. Methodology, feasibility, safety and diagnostic accuracy of dobutamine stress echocardiography. *J Am Coll Cardiol* 30: 595–606, 1997.

30. **La Gerche A**, **Claessen G**, **Van De Bruaene A**, **Pattyn N**, **Van Cleemput J**, **Gewillig M**, **Bogaert J**, **Dymarkowski S**, **Claus P**, **Heidbuchel H**. Cardiac MRI: A new gold standard for ventricular volume quantification during high-intensity exercise. *Circ Cardiovasc Imaging* 6: 329–338, 2013.

31. **La Gerche A**, **Gewillig M**. What Limits Cardiac Performance during Exercise in Normal Subjects and in Healthy Fontan Patients? *Int J Pediatr* 2010: 1–8, 2010.

32. **La Gerche A**, **Roberts T**, **Claessen G**. The response of the pulmonary circulation and right ventricle to exercise: exercise-induced right ventricular dysfunction and structural remodeling in endurance athletes (2013 Grover Conference series). *Pulm Circ* 4: 407–16, 2014.

33. **Geva T**. Repaired tetralogy of Fallot: the roles of cardiovascular magnetic resonance in evaluating pathophysiology and for pulmonary valve replacement decision support. *J Cardiovasc Magn Reson* 13: 9, 2011.

34. **Geva T**, **Martins JD**, **Wald RM**. Atrial septal defects. *Lancet* 383: 1921–32, 2014.

35. **Giardini A**, **Donti A**, **Formigari R**, **Specchia S**, **Prandstraller D**, **Bronzetti G**, **Bonvicini M**, **Picchio FM**. Determinants of cardiopulmonary functional improvement after transcatheter atrial septal defect closure in asymptomatic adults. *J Am Coll Cardiol* 43: 1886–1891, 2004.

36. **Giardini A**, **Donti A**, **Specchia S**, **Formigari R**, **Oppido G**, **Picchio FM**. Long-term impact of transcatheter atrial septal defect closure in adults on cardiac function and exercise capacity. *Int J Cardiol* 124: 179–82, 2008.

37. **Giardini A**, **Moore P**, **Brook M**, **Stratton V**, **Tacy T**. Effect of Transcatheter Atrial Septal Defect Closure in Children on Left Ventricular Diastolic Function. *Am J Cardiol* 95: 1255–1257, 2005.

38. **Gorter TM**, **Van Melle JP**, **Hillege HL**, **Pieper PG**, **Ebels T**, **Hoendermis ES**, **Bartelds B**, **Willems TP**, **Berger RMF**. Ventricular remodelling after pulmonary valve replacement: Comparison between pressure-loaded and volume-loaded right ventricles. *Interact Cardiovasc Thorac Surg* 19: 95–101, 2014.

39. **Gottdiener JS**, **Bednarz J**, **Devereux R**, **Gardin J**, **Klein A**, **Manning WJ**, **Morehead A**, **Kitzman D**, **Oh J**, **Quinones M**, **Schiller NB**, **Stein JH**, **Weissman NJ**. American Society of Echocardiography recommendations for use of echocardiography in clinical trials: A report from the american society of echocardiography's guidelines and standards committee and the task force on echocardiography in clinical trials. *J. Am. Soc. Echocardiogr.* 17: 1086–1119, 2004.

40. **Heiberg E**, **Pahlm-Webb U**, **Agarwal S**, **Bergvall E**, **Fransson H**, **Steding-Ehrenborg K**, **Carlsson M**, **Arheden H**. Longitudinal strain from velocity encoded cardiovascular magnetic resonance: a validation study. *J Cardiovasc Magn Reson* 15: 15, 2013.

41. **Helber U**, **Baumann R**, **Seboldt H**, **Reinhard U**, **Hoffmeister HM**. Atrial septal defect in adults: cardiopulmonary exercise capacity before and 4 months and 10 years after defect closure. *J Am Coll Cardiol* 29: 1345–1350, 1997.

42. **Hopkins WE**, **Waggoner AD**. Severe pulmonary hypertension without right ventricular failure: The unique hearts of patients with Eisenmenger syndrome. *Am J Cardiol* 89: 34–38, 2002.

43. **Jategaonkar S**, **Scholtz W**, **Schmidt H**, **Fassbender D**, **Horstkotte D**. Cardiac remodeling and effects on exercise capacity after interventional closure of atrial septal defects in different adult age groups. *Clin Res Cardiol* 99: 183–191, 2010.

44. **Kaul S**. The interventricular septum in health and disease. *Am Heart J* 112: 568–81, 1986.

45. **Kim JY**, **Yun B-S**, **Lee S**, **Jung SY**, **Choi JY**, **Kim NK**. Changes in Strain Pattern and Exercise Capacity after Transcatheter Closure of Atrial Septal Defects. *Korean Circ J* 47: 245, 2017.

46. **Kobayashi Y**, **Nakanishi N**, **Kosakai Y**. Pre- and postoperative exercise capacity associated with hemodynamics in adult patients with atrial septal defect: a retrospective study. *Eur J Cardiothorac Surg* 11: 1062–6, 1997.

47. **Kocica MJ**, **Corno AF**, **Carreras-Costa F**, **Ballester-Rodes M**, **Moghbel MC**, **Cueva CNC**, **Lackovic V**, **Kanjuh VI**, **Torrent-Guasp F**. The helical ventricular myocardial band: global, three-dimensional, functional architecture of the ventricular myocardium. *Eur J Cardio-thoracic Surg* 29, 2006.

48. **Komar M**, **Przewłocki T**, **Olszowska M**, **Sobień B**, **Tomkiewicz-Pająk L**, **Podolec P**. Is it worth closing the atrial septal defect in patients with insignificant shunt? *Postępy w Kardiol interwencyjnej = Adv Interv Cardiol* 10: 78–83, 2014.

49. **Kopic S**, **Stephensen SS**, **Heiberg E**, **Arheden H**, **Bonhoeffer P**, **Ersbøll M**, **Vejlstrup N**, **Søndergaard L**, **Carlsson M**. Isolated pulmonary regurgitation causes decreased right ventricular longitudinal function and compensatory increased septal pumping in a porcine model. *Acta Physiol.* .

50. **Kröönström LA**, **Johansson L**, **Zetterström A-K**, **Dellborg M**, **Eriksson P**, **Cider Å**. Muscle function in adults with congenital heart disease. *Int J Cardiol* 170: 358–363, 2014.

51. **Kuijpers D**, **Janssen CHC**, **van Dijkman PRM**, **Oudkerk M**. Dobutamine stress MRI. Part I. Safety and feasibility of dobutamine cardiovascular magnetic resonance in patients suspected of myocardial ischemia. *Eur Radiol* 14: 1823–1828, 2004.

52. **Levin AR**, **Spach MS**, **Boineau JP**, **Canent R V**, **Capp MP**, **Jewett PH**. Atrial pressure-flow dynamics in atrial septal defects (secundum type). *Circulation* 37: 476–88, 1968.

53. **van der Linde D**, **Konings EEM**, **Slager MA**, **Witsenburg M**, **Helbing WA**, **Takkenberg JJM**, **Roos-Hesselink JW**. Birth Prevalence of Congenital Heart Disease Worldwide. *J Am Coll Cardiol* 58: 2241–2247, 2011.

54. **Lu JC**, **Ghadimi Mahani M**, **Agarwal PP**, **Cotts TB**, **Dorfman AL**. Usefulness of Right Ventricular Free Wall Strain to Predict Quality of Life in "Repaired" Tetralogy of Fallot. *Am J Cardiol* 111: 1644–1649, 2013.

55. **Lundbäck S**. Cardiac pumping and function of the ventricular septum. *Acta Physiol Scand Suppl* 550: 1–101, 1986.

56. **Maagaard M**, **Heiberg J**, **Hjortdal VE**. Small, unrepaired ventricular septal defects reveal poor exercise capacity compared with healthy peers: A prospective, cohort study. *Int J Cardiol* 227: 631–634, 2017.

57. **Martin Bland J**, **Altman D**. Statistical Methods for Assessing Agreement Between Two Methods of Clinical Measurement. *Lancet* 327: 307–310, 1986.

58. **Masutani S**, **Senzaki H**. Left ventricular function in adult patients with atrial septal defect: Implication for development of heart failure after transcatheter closure. *J Card Fail* 17: 957–963, 2011.

59. **Masutani S**, **Taketazu M**, **Ishido H**, **Iwamoto Y**, **Yoshiba S**, **Matsunaga T**, **Kobayashi T**, **Senzaki H**. Effects of age on hemodynamic changes after transcatheter closure of atrial septal defect: importance of ventricular diastolic function. *Heart Vessels* 27: 71–78, 2012.

60. **Mertens LL**, **Friedberg MK**. Imaging the right ventricle—current state of the art. *Nat Rev Cardiol* 7: 551–563, 2010.

61. **Mertes H**, **Sawada SG**, **Ryan T**, **Segar DS**, **Kovacs R**, **Foltz J**, **Feigenbaum H**. Symptoms, adverse effects, and complications associated with dobutamine stress echocardiography. Experience in 1118 patients. *Circulation* 88: 15–19, 1993.

62. **Modesti PA**, **Vanni S**, **Bertolozzi I**, **Cecioni I**, **Lumachi C**, **Perna AM**, **Boddi M**, **Gensini GF**. Different Growth Factor Activation in the Right and Left Ventricles in Experimental Volume Overload. *Hypertension* 43: 101–108, 2004.

63. **Muzzarelli S**, **Ordovas KG**, **Cannavale G**, **Meadows AK**, **Higgins CB**. Tetralogy of Fallot: Impact of the Excursion of the Interventricular Septum on Left Ventricular Systolic Function and Fibrosis after Surgical Repair. *Radiology* 259: 375–383, 2011.

64. **Naeije R**, **Badagliacca R**. The overloaded right heart and ventricular interdependence. *Cardiovasc Res* 113: 1474–1485, 2017.

65. **Nollert G**, **Fischlein T**, **Bouterwek S**, **Böhmer C**, **Klinner W**, **Reichart B**. Long-Term Survival in Patients With Repair of Tetralogy of Fallot: 36-Year Follow-Up of 490 Survivors of the First Year After Surgical Repair. *J Am Coll Cardiol* 30: 1374–1383, 1997.

66. **Nonogi H**, **Hess OM**, **Ritter M**, **Krayenbuehl HP**. Diastolic properties of the normal left ventricle during supine exercise. *Br Heart J* 60: 30–38, 1988.

67. **Ostenfeld E**, **Stephensen SS**, **Steding-Ehrenborg K**, **Heiberg E**, **Arheden H**, **Rådegran G**, **Holm J**, **Carlsson M**. Regional contribution to ventricular stroke volume is affected on the left side, but not on the right in patients with pulmonary hypertension. *Int J Cardiovasc Imaging* 32: 1243–53, 2016.

68. **Pagnamenta, Alberto; Fesler, Pierre; Vandinivit, Alain; Brimioulle, Serge; Naeije R**. Pulmonary vascular effects of dobutamine in experimental pulmonary hypertension. *Crit Care Med* 31: 1140–1146, 2003.

69. **Parish V**, **Valverde I**, **Kutty S**, **Head C**, **Qureshi S a**, **Sarikouch S**, **Greil G**, **Schaeffter T**, **Razavi R**, **Beerbaum P**. Dobutamine stress MRI in repaired tetralogy of Fallot with chronic pulmonary regurgitation: a comparison with healthy volunteers. *Int J Cardiol* 166: 96–105, 2013.

70. **Pascotto M**, **Santoro G**, **Cerrato F**, **Caputo S**, **Bigazzi MC**, **Iacono C**, **Carrozza M**, **Russo MG**, **Caianiello G**, **Calabrò R**. Time-course of cardiac remodeling following transcatheter closure of atrial septal defect. *Int J Cardiol* 112: 348–352, 2006.

71. **Pettersen E**, **Helle-Valle T**, **Edvardsen T**, **Lindberg H**, **Smith HJ**, **Smevik B**, **Smiseth OA**, **Andersen K**. Contraction Pattern of the Systemic Right Ventricle. Shift From Longitudinal to Circumferential Shortening and Absent Global Ventricular Torsion. *J Am Coll Cardiol* 49: 2450–2456, 2007.

72. **Pfammatter J-P**, **Zanolari M**, **Schibler A**. Cardiopulmonary exercise parameters in children with atrial septal defect and increased pulmonary blood flow: short-term effects of defect closure. *Acta Paediatr* 91: 65–70, 2007.

73. **Pollick C**, **Sullivan H**, **Cujec B**, **Wilansky S**. Doppler color-flow imaging assessment of shunt size in atrial septal defect. *Circulation* 78: 522–8, 1988.

74. **Popp R**, **Wolfe S**, **Hirata T**, **Feigenbaum H**. Estimation of Right and Left Ventricular Size by Ultrasound. *Am J Cardiol* 24: 523–530, 1969.

75. **Rhodes J**, **Patel H**, **Hijazi ZM**. Effect of transcatheter closure of atrial septal defect on the cardiopulmonary response to exercise. *Am J Cardiol* 90: 803–806, 2002.

76. **Riesenkampff E**, **Al-Wakeel N**, **Kropf S**, **Stamm C**, **Alexi-Meskishvili V**, **Berger F**, **Kuehne T**. Surgery impacts right atrial function in tetralogy of Fallot. *J Thorac Cardiovasc Surg* 147: 1306–1311, 2014.

77. **Roeleveld RJ**, **Marcus JT**, **Faes TJC**, **Gan T-J**, **Boonstra A**, **Postmus PE**, **Vonk-Noordegraaf A**. Interventricular septal configuration at mr imaging and pulmonary arterial pressure in pulmonary hypertension. *Radiology* 234: 710–717, 2005.

78. **Rudski LG**, **Lai WW**, **Afilalo J**, **Hua L**, **Handschumacher MD**, **Chandrasekaran K**, **Solomon SD**, **Louie EK**, **Schiller NB**. Guidelines for the Echocardiographic Assessment of the Right Heart in Adults: A Report from the American Society of Echocardiography. *J Am Soc Echocardiogr* 23: 685–713, 2010.

79. **Rutz T**, **Ghandour F**, **Meierhofer C**, **Naumann S**, **Martinoff S**, **Lange R**, **Ewert P**, **Stern HC**, **Fratz S**. Evolution of right ventricular size over time after tetralogy of Fallot repair: A longitudinal cardiac magnetic resonance study. *Eur Heart J Cardiovasc Imaging* 18: 364–370, 2017.

80. **Ryan T**, **Petrovic O**, **Dillon JC**, **Feigenbaum H**, **Conley MJ**, **Armstrong WF**. An echocardiographic index for separation of right ventricular volume and pressure overload. *J Am Coll Cardiol* 5: 918–924, 1985.

81. **S A Rebergen, J G Chin, J Ottenkamp, E E van der Wall A de R**. Pulmonary regurgitation in the late postoperative follow-up of tetralogy of Fallot. Volumetric quantitation by nuclear magnetic resonance velocity mapping. *Circulation* 88, 1993.

82. **Sallin EA**. Fiber orientation and ejection fraction in the human left ventricle. *Biophys J* 9: 954–64, 1969.

83. **Santos M**, **Systrom D**, **Epstein SE**, **John A**, **Ruiz G**. Impaired exercise capacity

following atrial septal defect closure : an invasive study of the right heart and pulmonary circulation. *Pulm Circ* 4: 630–637, 2014.

84. **Satoh A**, **Katayama K**, **Hiro T**, **Yano M**, **Miura T**, **Kohno M**, **Fujii T**, **Matsuzaki M**. Effect of right ventricular volume overload on left ventricular diastolic function in patients with atrial septal defect. *Jpn Circ J* 60: 758–766, 1996.

85. **Schoen SP**, **Kittner T**, **Bohl S**, **Braun MU**, **Simonis G**, **Schmeisser A**, **Strasser RH**, **Schoen SP**. Transcatheter closure of atrial septal defects improves right ventricular volume, mass, function, pulmonary pressure, and functional class: a magnetic resonance imaging study. *Heart* 92: 821–826, 2006.

86. **Secknus MA**, **Marwick TH**. Evolution of dobutamine echocardiography protocols and indications: Safety and side effects in 3,011 studies over 5 years. *J Am Coll Cardiol* 29: 1234–1240, 1997.

87. **Smerup M**, **Nielsen E**, **Agger P**, **Frandsen J**, **Vestergaard-Poulsen P**, **Andersen J**, **Nyengaard J**, **Pedersen M**, **Ringgaard S**, **Hjortdal V**, **Lunkenheimer PP**, **Anderson RH**. The three-dimensional arrangement of the myocytes aggregated together within the mammalian ventricular myocardium. *Anat Rec* 292: 1–11, 2009.

88. **Steding-Ehrenborg K**, **Carlsson M**, **Stephensen S**, **Arheden H**. Atrial aspiration from pulmonary and caval veins is caused by ventricular contraction and secures 70% of the total stroke volume independent of resting heart rate and heart size. *Clin Physiol Funct Imaging* 33: 233–240, 2013.

89. **Steding-Ehrenborg K**, **Jablonowski R**, **Arvidsson PM**, **Carlsson M**, **Saltin B**, **Arheden H**. Moderate intensity supine exercise causes decreased cardiac volumes and increased outer volume variations: a cardiovascular magnetic resonance study. *J Cardiovasc Magn Reson* 15: 96, 2013.

90. **Stephensen S**, **Steding-Ehrenborg K**, **Munkhammar P**, **Heiberg E**, **Arheden H**, **Carlsson M**. The relationship between longitudinal, lateral, and septal contribution to stroke volume in patients with pulmonary regurgitation and healthy volunteers. *Am J Physiol Heart Circ Physiol* 306: H895-903, 2014.

91. **Stephensen SS**, **Ostenfeld, Ellen. Steding-Ehrenborg, Katarina. Thilén, Ulf. Heiberg, Einar. Arheden, Hakan. Carlsson M**. *Alterations in ventricular pumping in patients with atrial septal defect at rest, during dobutamine stress and after defect closure (submitted)*. 2017.

92. **Stephensen SS**, **Steding-Ehrenborg K**, **Thilén U**, **Holm J**, **Hochbergs P**, **Arheden H**, **Carlsson M**. Changes in blood volume shunting in patients with atrial septal defects: assessment of heart function with cardiovascular magnetic resonance during dobutamine stress. *Eur Hear J - Cardiovasc Imaging* Sep 1. doi, 2016.

93. **Stirrat J**, **Rajchl M**, **Bergin L**, **Patton DJ**, **Peters T**, **White JA**. High-resolution 3-dimensional late gadolinium enhancement scar imaging in surgically corrected Tetralogy of Fallot: clinical feasibility of volumetric quantification and visualization. *J Cardiovasc Magn Reson* 16: 76, 2014.

94. **Su CT**, **Sung TY**, **Lin KL**, **Wang JL**, **Yang AL**. Lower exercise capacity in children with asymptomatic atrial septal defect associated with circulatory impairment. *Chin J Physiol* 56, 2013.

95. **Suchon E**, **Podolec P**, **Tomkiewicz-Pajak L**, **Kostkiewicz M**, **Mura A**, **Pasowicz**

M, **Tracz W**. Cardiopulmonary exercise capacity in adult patients with atrial septal defect. *Przegl Lek* 59: 747–751, 2002.

96. **Suchon E**, **Tracz W**, **Podolec P**, **Sadowski J**. Atrial septal defect in adults: echocardiography and cardiopulmonary exercise capacity associated with hemodynamics before and after surgical closure. *Interact Cardiovasc Thorac Surg* 4: 488–492, 2005.

97. **Thadani U**, **West RO**, **Mathew TM**, **Parker JO**. Hemodynamics at rest and during supine and sitting bicycle exercise in patients with coronary artery disease. *Am J Cardiol* 39: 776–783, 1977.

98. **Thilén U**, **Persson S**. Closure of atrial septal defect in the adult. Cardiac remodeling is an early event. *Int J Cardiol* 108: 370–375, 2006.

99. **Tuttle RR**, **Mills J**. Dobutamine: development of a new catecholamine to selectively increase cardiac contractility. *Circ Res* 36: 185–196, 1975.

100. **Ugander M**, **Carlsson M**, **Arheden H**. Short-axis epicardial volume change is a measure of cardiac left ventricular short-axis function, which is independent of myocardial wall thickness. *Am J Physiol Heart Circ Physiol* 298: H530-5, 2010.

101. **van de Veerdonk MC**, **Bogaard HJ**, **Voelkel NF**. The right ventricle and pulmonary hypertension. *Heart Fail Rev* 21: 259–271, 2016.

102. **Villafañe J**, **Feinstein JA**, **Jenkins KJ**, **Vincent RN**, **Walsh EP**, **Dubin AM**, **Geva T**, **Towbin JA**, **Cohen MS**, **Fraser C**, **Dearani J**, **Rosenthal D**, **Kaufman B**, **Graham TP**. Hot topics in tetralogy of fallot. *J Am Coll Cardiol* 62: 2155–2166, 2013.

103. **Voelkel NF**, **Quaife RA**, **Leinwand LA**, **Barst RJ**, **McGoon MD**, **Meldrum DR**, **Dupuis J**, **Long CS**, **Rubin LJ**, **Smart FW**, **Suzuki YJ**, **Gladwin M**, **Denholm EM**, **Gail DB**. Right ventricular function and failure: Report of a National Heart, Lung, and Blood Institute working group on cellular and molecular mechanisms of right heart failure. *Circulation* 114: 1883–1891, 2006.

104. **Wasserman, K.; Hansen, J. E.; Sue, D. Y.; Stringer, W. W.; Sietsema, K. E.; Sun, X. G.; Whipp BJ**. Principles of exercise testing and interpretation: including pathophysiology and clinical application. Baltimore, Maryland, USA: Lippincott Williams & Wilkins, 2004.

105. **Weyman a E**, **Wann S**, **Feigenbaum H**, **Dillon JC**. Mechanism of abnormal septal motion in patients with right ventricular volume overload: a cross-sectional echocardiographic study. *Circulation* 54: 179–186, 1976.

106. **Zaffran S**, **Kelly RG**, **Meilhac SM**, **Buckingham ME**, **Brown NA**. Right ventricular myocardium derives from the anterior heart field. *Circ Res* 95: 261–268, 2004.

Acknowledgements

I would like to thank the people who have, in one way or another, helped me claw my way through the grueling years as a PhD student.

Marcus Carlsson my supervisor for teaching me about the physiology of the heart, cardiac MRI, how to write a scientific paper and providing good advice on child rearing.

My co-supervisors Ellen Ostenfeld and Håkan Arheden for their support and enlightening discussions and Ulf Thilén for opening my eyes to the world of grown-ups with congenital heart defects.

The cardiac MR group in Lund for giving me the opportunity to work in such a disciplined and innovative environment. Especially Katarina Steding-Ehrenborg for feedback and contribution to my papers and Einar Heiberg for providing new parameter for Segment on as-needed basis.

The MRI technicians Ann-Helen Arvidsson, Christel Carlander and Lotta Åkesson for recruiting patients and collecting all the data.

My colleagues at the department of pediatric cardiology, Katarina Hanséus, Gudrun Björkhem, Petru Liuba, Nina Hacacova, Ida Jeremiasen, Rita Janusauskaite, Yahia Elmahdi, Petru Liuba, Thomas Higgins and last but not least Peter Munkhammer for introducing me to the work of the cardiac MR group in Lund.

My brother and sister Eiríkur and Sigga. My wonderful companion Kata who has taught me it's okay to be optimistic. My stepdaughter Sóley and my 3 month old daughter, with whom I look forward to spend more time.

The studies were supported by the Region of Skåne, the Swedish Heart-Lung Foundation, the Swedish Medical Association, Lund University and the Swedish Research Council.

Printed by Media-Tryck, Lund 2017 NORDIC ECOLABEL, 3041 0903

Sigurður Sverrir Stephensen is born in Uppsala on November 1st 1968. He graduated from medical school in Iceland in 1997. He did his residency in general pediatrics at the at CT Children's Medical Center in Hartford, USA and his fellowship in pediatric cardiology at Skånes University Hospital in Lund. He is currently working at the Children's Hospital in Reykjavík, Iceland. His inspiration in life and fashion is David Attenborough.

LUND UNIVERSITY
Faculty of Medicine

Department of Clinical Physiology

Lund University, Faculty of Medicine
Doctoral Dissertation Series 2017:182
ISBN 978-91-7619-564-2
ISSN 1652-8220

9 789176 195642